[HRh(CO)$_4$]-Catalyzed Hydrogenation of Co: A Systematic Ab Initio Quantum-Chemical Investigation of the Reaction Mechanism**

Ulrich Pidun and Gernot Frenking*

Abstract: The mechanism of the [HRh(CO)$_4$]-catalyzed hydrogenation of carbon monoxide has been studied with the help of ab initio quantum-chemical calculations at the MP2 level of theory. A quasirelativistic effective core potential was used at rhodium in combination with valence basis sets of double-zeta quality with additional polarization functions. A systematic and unbiased approach has been followed: In the first part of the investigation, for each intermediate of the postulated catalytic mechanism all stable conformations were determined and characterized as minima on the potential energy surface by calculation of the energy Hessian. In the geometry optimizations all theoretically reasonable structures were taken into account (up to 32 starting structures per intermediate) and not just those which fit well into the proposed mechanism. In the second part of the work, the calculated energy-minimum structures were integrated into the catalytic mechanism and the transition states for the individual reaction steps were determined and characterized by calculation of the intrinsic reaction coordinate (IRC) connecting them with the corresponding energy-minimum structures. In spite of this unbiased approach, a rather simple and very smooth reaction profile for the catalytic mechanism is found, without thermodynamic traps or insurmountable barriers. The first step of the catalysis, the formation of the formyl complex [(HCO)Rh(CO)$_3$] from the starting catalyst [HRh(CO)$_4$], is the rate-determining step of the whole reaction and thus responsible for the requirement of high temperature and pressure. The details of the calculated mechanism help to understand a number of experimental observations and answer several questions discussed in the literature. Furthermore, the presented results might serve as a basis for a rational improvement of the catalyst systems currently in use.

Keywords: ab initio calculations · carbon monoxide · homogeneous catalysis · hydrogenations · rhodium

Introduction

Facing declining resources of mineral oil and natural gas, chemical research is increasingly urged to find alternative sources of carbon for the large-scale production of chemical compounds. A possible approach for the synthesis of compounds of the type $C_xH_yO_z$ is the controlled hydrogenation of carbon monoxide, which is readily available from coal. The first processes of this kind date back to the Second World War, when German scientists developed heterogeneously catalyzed methods for the production of synthetic fuel (Fischer–Tropsch process). Later on, South Africa further improved these processes (SASOL) under the pressure of the embargo of the apartheid regime. These classical methods for CO hydrogenation employ heterogeneous catalysts. The selectivities, however, are rather poor.

The breathtaking development of organometallic chemistry has now pushed homogeneous variants of the catalytic CO hydrogenation into the focus of research interest.[1] Homogeneous catalysts simplify the study of the reaction mechanisms, so a rational design of the catalysts should be possible in principle. It turned out that homogeneous rhodium catalysts are particularly suited for the synthesis of simple oxygenated products like formaldehyde, methanol, acetic acid or ethylene glycol. There are two principal approaches: Either the oxo products are directly obtained from a mixture of CO and H_2,[2] or in an indirect process C_1 products are first built from synthesis gas in a separated reaction and afterwards are treated with CO and H_2 to give the desired C_2 products.[3] There are a number of well-established processes of the indirect type, the most prominent being probably the Monsanto acetic acid synthesis.[3–7] Further examples for well-investigated indirect processes of CO hydrogenation are the competing hydroformylation and hydrogenation of formaldehyde[2, 4, 6, 8] and the homologation of methanol to ethanol by transformation with mixtures of CO and H_2.[3, 9]

[*] Prof. Dr. G. Frenking, Dr. U. Pidun
Fachbereich Chemie der Philipps-Universität Marburg
Hans-Meerwein-Strasse, D-35032 Marburg (Germany)
Fax: (+ 49) 6421-282189
E-mail: frenking@ps1515.chemie.uni-marburg.de

[**] Theoretical Studies of Organometallic Compounds, Part 28. Part 27: Ref. [26b].

0947-6539/98/0403-0522 $ 17.50+.50/0 *Chem. Eur. J.* **1998**, *4*, No. 3

Direct homogeneously catalyzed procedures for the synthesis of oxygenated C_2 products by hydrogenation of CO have also been intensively studied but have not led to any large-scale industrial applications yet. The most carefully investigated process is certainly the Union Carbide method for the conversion of CO and H_2 to ethylene glycol.[4, 10–12] Soluble rhodium carbonyl complexes turned out to be the most effective catalysts and a number of additives, like basic phosphines, amide solvents, nitrogen bases and alkali cations, were tested in order to further increase reaction rates and selectivities.[2, 13–17] However, in spite of these large research expenses, only gradual improvements of the catalytic process of ethylene glycol formation could be achieved. The same holds for the other direct procedures of homogeneously catalyzed hydrogenation of carbon monoxide, like synthesis of methanol or methyl formate.[2] It was concluded that for a systematic development of effective catalysts for CO hydrogenation reactions a better understanding of the fundamental mechanistic processes is inevitable.[1]

Little is known experimentally about intermediates and reaction steps of the catalytic hydrogenation of carbon monoxide. However, it is generally believed that similar intermediates and reaction pathways play the dominant role in the different procedures, that is, that there are fundamental mechanistic principles underlying all catalytic processes discussed.[4] A number of reaction intermediates and single steps have been postulated that are in accord with experimental observations. However, a true experimental proof has not yet been provided.[2] In earlier work, the idea of a dual coordination of the CO molecule at two metal centres had been favoured.[18] Today, it is generally accepted that the actual catalysis takes place at a mononuclear rhodium centre.[2] $[HRh(CO)_4]$ and its substituted derivatives are mostly supposed to be the active catalytic species. The occurrence of formaldehyde—either as a free molecule or in the coordinated form—in the course of the reaction is also widely accepted.[2] Further intermediates that have been proposed on the basis of experimental observations are formyl complexes $[(HCO)RhL_n]$,[2, 6, 18–20] hydroxycarbene complexes $[(HOCH)RhL_n]$,[18, 20, 21] hydroxymethyl complexes $[(OHCH_2)RhL_n]$[2, 22] and methoxy complexes $[(CH_3O)RhL_n]$.[2] Since direct experimental evidence for these intermediates is absent, their occurrence is rather speculative.

At this point of development, quantum-chemical methods should be a useful tool for a further clarification of the underlying mechanistic principles of the catalytic hydrogenation of carbon monoxide. In the last decade, progress in ab initio quantum chemistry has permitted its application not just to elementary steps of organometallic reactions, but to entire catalytic cycles. The models for the reacting complexes become more and more realistic and the applied theoretical methods are continuously refined. In this way, quantum-chemical calculations provide valuable information on structures and energies of intermediates and transition states of catalytic reactions, in particular when combined with experimental results.[23–26] The performance of modern ab initio quantum chemistry for the description of organometallic reaction mechanisms has been compiled in several review articles.[27–30]

Surprisingly, the apparently simple mechanism of Rh-catalyzed CO hydrogenation has not yet been the subject of a systematic quantum-chemical investigation. In 1988 Sgamellotti and Floriani investigated some intermediates of the CO hydrogenation catalyzed by $[Fe(CO)_2(PH_3)_2]$ at the Hartree–Fock level of theory.[31] However, they had to fix the geometry of the $[Fe(CO)_2(PH_3)_2]$ fragment in the various complexes and could perform only partial optimizations. An ab initio study of the CO insertion into the bare Rh–H bond has been carried out by Siegbahn et al.[32] In 1991 Koga and Morokuma published an ab initio MO study on the C–C bond-forming reaction in the dinuclear Rh complex $[(CpRh)_2(\mu\text{-}CH_2)_2(CH_3)H]$, which might serve as a model for the Fischer–Tropsch C–C coupling on rhodium surfaces.[33] Although the theoretical level chosen should not allow any quantitative statements, they found that the coupling of two alkyl groups is clearly favoured when catalyzed by a dinuclear Rh complex as compared to a mononuclear catalyst. Versluis and Ziegler used density-functional theory (DFT) to investigate a possible reaction step of the catalytic hydrogenation of CO, the insertion of a CH_2O molecule into a metal–hydrogen bond, using the complex $[HCo(CO)_3]$.[34] They located a π complex between formaldehyde and $HCo(CO)_3$ that can rearrange either to a methoxy complex or to a hydroxymethyl complex. The higher stability of the methoxy complex was explained by the oxophilicity of cobalt. Finally, three Chinese studies should be mentioned that try to describe the mechanistic details of heterogeneously catalyzed CO hydrogenations with the semiempirical Extended Hückel theory (EHT).[35–37] Even though the experimental sequence of reactivity of various transition metals and the effect of different additives are theoretically well reproduced, the fact should not be overlooked that the EHT method is certainly not appropriate for this kind of problems and that the claimed good results are rather fortuitous.

No further theoretical studies dealing explicitly with the catalytic hydrogenation of carbon monoxide could be found in the literature. So we decided to carry out a systematic ab initio quantum-chemical investigation of the mechanism of the CO hydrogenation reaction homogeneously catalyzed by rhodium complexes. A general mechanism has to explain the formation of several fragments that are found in the products of the reaction, including the formyl and acetyl group, the fragments $HOCH_2$- and CH_3O-, and the formaldehyde molecule, whose formation is widely accepted by now. Furthermore, a careful theoretical study should give answers to a number of concrete questions that have been raised by earlier investigations of this reaction:

Is the direct formation of formyl complexes from hydridocarbonyl complexes possible? Does it occur by H migration to the carbonyl ligand or by CO insertion into the Rh–H bond?

Are formyl complexes stabilized by μ^2-coordination?

If H_2 is added to the catalyst, is the dihydrido complex directly formed or is there a nonclassical dihydrogen complex as intermediate?

Does the mechanism follow the formaldehyde or the hydroxycarbene route?

How is formaldehyde coordinated to the Rh complex: side-on or end-on?

Are the hydroxymethyl or the methoxy intermediates preferred?

Which reaction step requires the high temperatures and pressures known to be necessary?

Figure 1 shows a proposed mechanism for the CO hydrogenation catalyzed by $[HRh(CO)_4]$. The mechanism accounts for the results of earlier studies of this reaction as well as for the important intermediates and reaction steps discussed in the literature. It starts with $[HRh(CO)_4]$ (**1**) as the catalytically active species that may rearrange either by H migration or by CO insertion to the formyl complex **2**. This unsaturated species can add H_2 to yield **3**, and eventually form the dihydrido complex **4** that may rearrange to the formaldehyde species **5** or to the hydroxycarbene complex **6**. Complex **5** can further react to the methoxy complex **8** or to the hydroxymethyl complex **7**, which can also be formed from the hydroxycarbene **6**. Species **7** and **8** can further add H_2 or CO and serve as intermediates for the formation of methanol, C_2 alcohols, methyl ethers and methyl esters. The observation of formaldehyde in the reaction mixture might be explained by the loss of the CH_2O ligand from **5** or by direct formation from the formyldihydrido complex **4**.

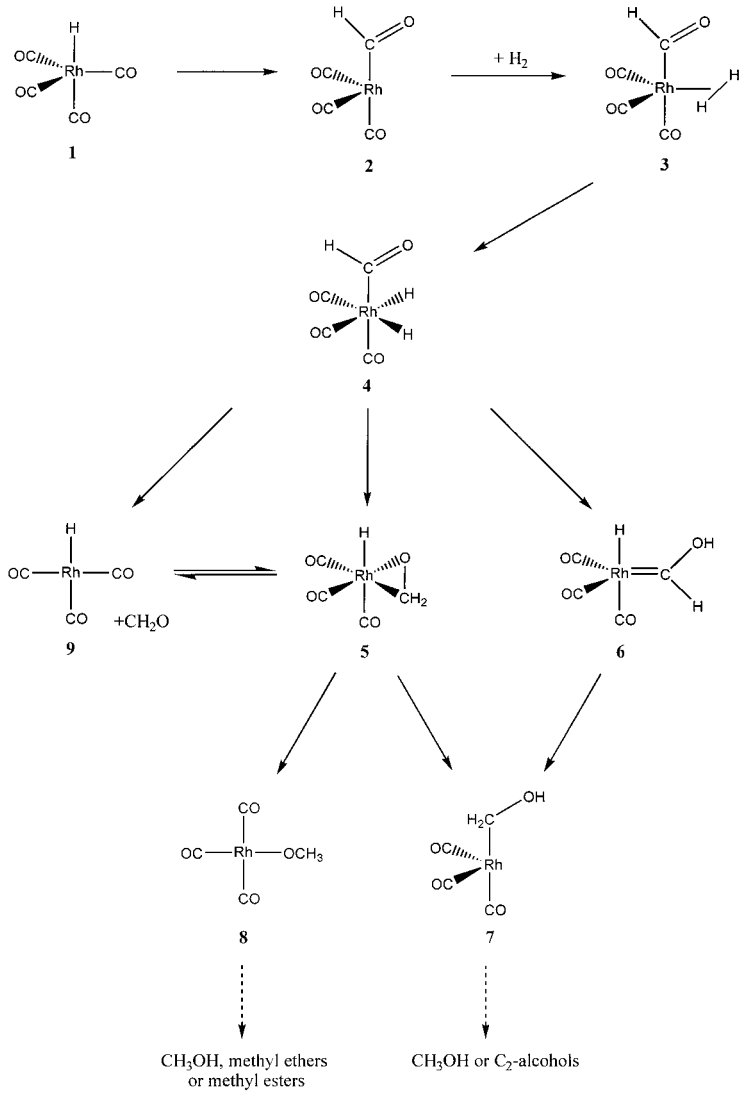

Figure 1. Proposed mechanism for the hydrogenation of CO catalyzed by $[HRh(CO)_4]$.

In the present study, the proposed mechanism in Figure 1 is systematically investigated with the help of ab initio quantum-chemical techniques. Only the singlet potential energy surface has been studied, because it is very likely that the supposed $Rh^{I}(d^8)$ and $Rh^{III}(d^6)$ complexes have a closed-shell electronic configuration. We want to point out that the present work does not cover the whole catalytic cycle of CO hydrogenation, but rather stops at the formation of the methoxy or hydroxymethyl intermediate. This means that the initial reaction steps which lead to the entrance channels for the different products have been studied, which give the most important information about the reaction course. As a first step, the stable conformers of the postulated intermediates were detected and confirmed as true minima on the potential energy surface. The minima were further characterized by the calculation of rotational barriers for the various ligands. In the second part of the work the transition states between the energy minima were located and characterized by calculation of their energy Hessian and the intrinsic reaction coordinates leading to the corresponding minima. In this way, a complete reaction profile for the proposed mechanism could be obtained that allows conclusions about the preferred reaction pathways and rate-determining steps.

A main characteristic of the present work is a systematic and unbiased approach. For each intermediate all theoretically reasonable conformations were considered in the geometry optimizations, irrespective of their structural fitting into the mechanism and of the optimized geometries of the preceding intermediates. No restrictions based on chemical intuition were made. In this way, up to 32 starting structures per intermediate have been considered in the geometry optimizations; these structures are given as supporting information.

Computational Methods

The geometries of the intermediates and transition states of the catalytic mechanism have been optimized at the MP2 (Møller–Plesset perturbation theory terminated at second order)[38] level of theory. For each postulated intermediate all possible conformations that cannot easily be rearranged into each other by simple bending were taken into account as starting structures (up to 32 per intermediate). In particular, there were always several structures without any symmetry. The starting structures for the geometry optimizations are given as supporting information. All the stationary points found were characterized by numerical calculation of the energy Hessian at the MP2 level of theory. A further characterization of the transition states was achieved by calculation of the intrinsic reaction coordinate (IRC)[39–43] at the MP2 level leading to the corresponding energy minima. The harmonic vibrational frequencies and corrections to the zero-point vibrational energy were also calculated at the MP2 level of theory; all frequencies are unscaled.

For the lighter elements H, C and O all-electron 6-31G(d,p) standard basis sets[44] were used. The rhodium atom was described

0947-6539/98/0403-0524 $ 17.50+.50/0 *Chem. Eur. J.* **1998**, *4*, No. 3

by a quasirelativistic small-core pseudopotential developed by Hay and Wadt.[45, 46] The 4s, 4p, 4d and 5s electrons are treated explicitly. The corresponding valence basis set is of double-zeta quality with a contraction (441/2111/31). These basis sets and pseudopotentials (denoted as basis set II) have proven to be very appropriate for the description of transition metal complexes, in particular when combined with the MP2 method for the geometry optimizations.[47]

The calculations were carried out with the program packages Turbomole,[48] Gaussian 92[49] and Gaussian 94.[50] For selected complexes a further investigation of the electronic structure was performed with the charge decomposition analysis (CDA) developed by Dapprich and Frenking.[51]

Results and Discussion

The presentation and discussion of the results is organized in the following way. First, we present the results of the geometry optimizations for the individual intermediates of the postulated catalytic mechanism of Figure 1. Subsequently, we will investigate how the energy-minimum structures fit into the mechanism and which thermodynamic profile results for the reaction sequence. Finally, the transition states connecting the calculated intermediates are presented and the complete reaction profile of the proposed mechanism is discussed.

1. Intermediates of the catalytic mechanism: Figure 2 shows the optimized geometries of the energy-minimum conformations for the individual intermediates of the postulated catalytic mechanism. Energies are given relative to the most stable conformer for each intermediate. The complete geometrical data as well as total energies and zero-point vibrational energy corrections are available as supporting information.

[HRh(CO)$_4$] (1): For the starting molecule [HRh(CO)$_4$] of the proposed catalytic mechanism, three possible geometries are discussed in the literature: a trigonal bipyramidal structure with axial (C_{3v}) or equatorial (C_{2v}) hydride ligand and a quadratic pyramidal structure with apical H (C_{4v}). However, the systematic geometry optimizations resulted in only one energy-minimum structure **1**, shown in Figure 2. The calculated structure is in qualitative agreement with the only published experimental characterization of [HRh(CO)$_4$]: from a comparison of the IR spectra of [HRh(CO)$_4$] and [HCo(CO)$_4$] Vidal and Walker proposed that the rhodium complex should have a C_{3v} symmetric structure.[52] Jonas and Thiel could also establish the C_{3v} form of [HRh(CO)$_4$] as an energy minimum.[53] Using various theoretical methods (HF, MP2, BP86) and two different basis sets, they found geometries very similar to the one shown in Figure 2. However, these authors did not consider any symmetries other than C_{3v}. The present work shows that the C_{4v} structure does not exist as a stationary point on the potential energy surface, while the C_{2v} symmetric trigonal bipyramidal form with an equatorial hydride ligand corresponds to the transition state of the degenerate Berry pseudorotation connecting two C_{3v} minimum structures. The activation energy of this pseudorotation amounts to 13.4 kcal mol^{-1}.

[(HCO)Rh(CO)$_3$] (2): The formyl complex **2**, corresponding to the second stage of the catalytic mechanism, might have a planar structure or a geometry derived from a trigonal bipyramid with one free coordination site. Considering all possible relative arrangements of the ligands, twelve starting structures have been taken into account in the geometry optimizations. Nevertheless, only two energy-minimum structures **2a** and **2b** are found (Figure 2). Both structures are energetically very similar, and **2b** should be obtained from **2a** by simply bending one of the carbonyl groups and simultaneously forming a stabilizing interaction between the formyl oxygen atom and the Rh centre. This μ^2-coordination of the formyl group lengthens the formyl C–O bond from 1.178 Å to 1.209 Å. The energetic similarity of **2a** and **2b** indicates that a μ^2-coordination is possible in formyl complexes, but that it is not indispensable for their stabilization. An interesting difference between **2a** and **2b** is observed upon rotation of the formyl group: In **2a** the CHO ligand rotates virtually freely, with a barrier of only 0.2 kcal mol^{-1}, while the rotation of the formyl group in **2b** results in a migration of the hydride ligand to the rhodium centre yielding **1** as soon as the H atom approaches the empty coordination site at Rh. This might serve as a first hint at the experimentally known inherent instability of coordinatively unsaturated formyl complexes with respect to a rearrangement to hydridocarbonyl complexes. Accordingly, the intermediate **2a** is less stable than the starting catalyst **1** by 28.2 kcal mol^{-1}, a fact that will be further discussed in the following sections.

[(HCO)Rh(CO)$_3$(H$_2$)] (3): The addition of H_2 to the coordinatively unsaturated complex **2** leads to the nonclassical dihydrogen complex **3**. For this intermediate 20 possible conformers were considered in the geometry optimizations, differing in the relative positions of the formyl and H_2 ligand in the coordination sphere of the rhodium centre (see supporting information). In spite of the large number of starting structures only three minimum geometries are found on the potential energy surface (**3a**–**c**, Figure 2). All three minima have a trigonal bipyramidal structure with the formyl group in the axial position. In **3a** the dihydrogen ligand occupies the axial site *trans* to the formyl group, while it is in an equatorial position in **3b** and **3c**. Thus, **3b** and **3c** differ only by rotation of the formyl ligand. The three isomers are very similar in energy: **3a** is about 1 kcal mol^{-1} more stable than **3b** and **3c**, which differ only by 0.1 kcal mol^{-1}.

The Rh–H_2 bonding interaction is weakest in the axial position (**3a**), the Rh–H distance amounts to 2.021 Å and the H–H bond is only lengthened from 0.734 Å in free H_2 to 0.771 Å in the complex. A surprisingly big difference is found in the Rh–H_2 bonding between the two rotamers **3b** and **3c**. In **3b** the H_2 molecule is very tightly coordinated with an Rh–H distance of 1.851 Å and an H–H bond length of 0.814 Å. In **3c** the Rh–H_2 interaction is still strong, but the Rh–H distance is 0.025 Å longer than in **3b**. The Rh centre in **3c** acts as a weaker Lewis acid as compared to **3b**, because the H_2 ligand has to compete with the formyl oxygen lone pairs for the free coordination site at the metal. Note the nice correlation between the strength of the Rh–H_2 interaction and the H–H bond length: the shorter the Rh–H distance, the more the H–H bond of the coordinating H_2 molecule is elongated.

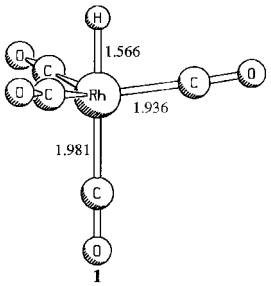

1

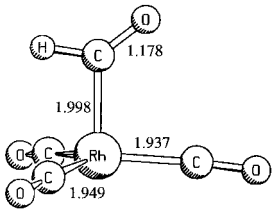

2a

E_{rel} = 0.0 kcal mol^{-1}

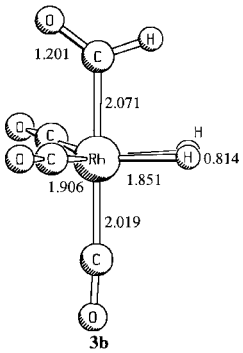

3b

E_{rel} = +1.0 kcal mol^{-1}

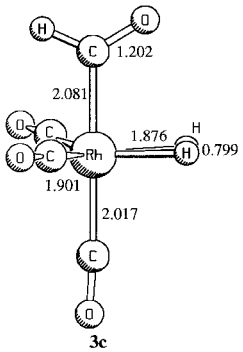

3c

E_{rel} = +1.1 kcal mol^{-1}

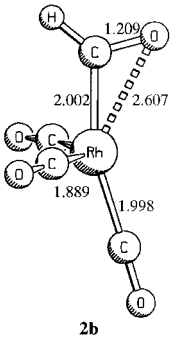

2b

E_{rel} = +1.3 kcal mol^{-1}

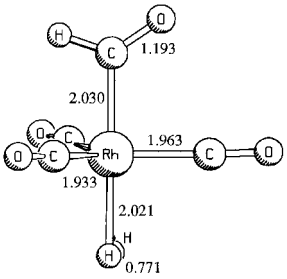

3a

E_{rel} = 0.0 kcal mol^{-1}

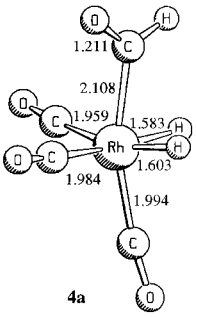

4a

E_{rel} = 0.0 kcal mol^{-1}

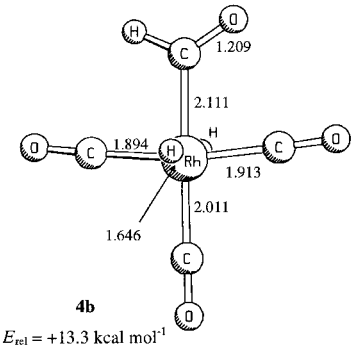

4b

E_{rel} = +13.3 kcal mol^{-1}

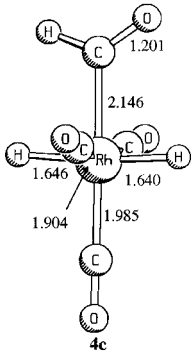

4c

E_{rel} = +13.5 kcal mol^{-1}

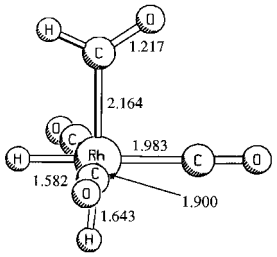

4d

E_{rel} = +13.6 kcal mol^{-1}

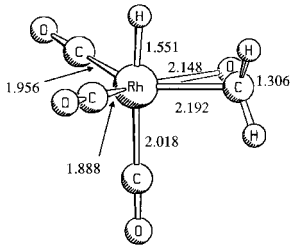

5a

E_{rel} = 0.0 kcal mol^{-1}

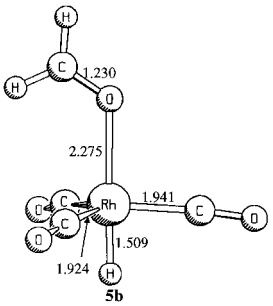

5b

E_{rel} = +3.8 kcal mol^{-1}

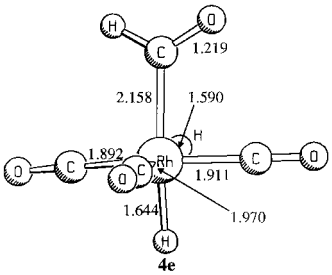

4e

E_{rel} = +14.2 kcal mol^{-1}

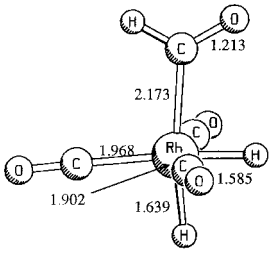

4f

E_{rel} = +14.3 kcal mol^{-1}

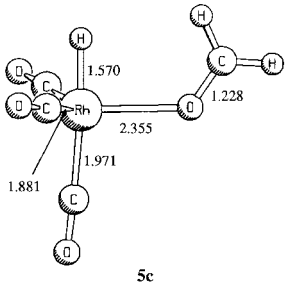

5c

E_{rel} = +4.9 kcal mol^{-1}

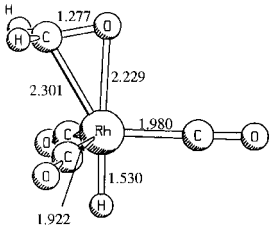

5d

E_{rel} = +5.3 kcal mol^{-1}

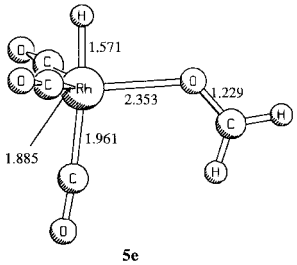

5e

E_{rel} = +5.4 kcal mol^{-1}

0947-6539/98/0403-0526 $ 17.50+.50/0 *Chem. Eur. J.* **1998**, *4*, No. 3

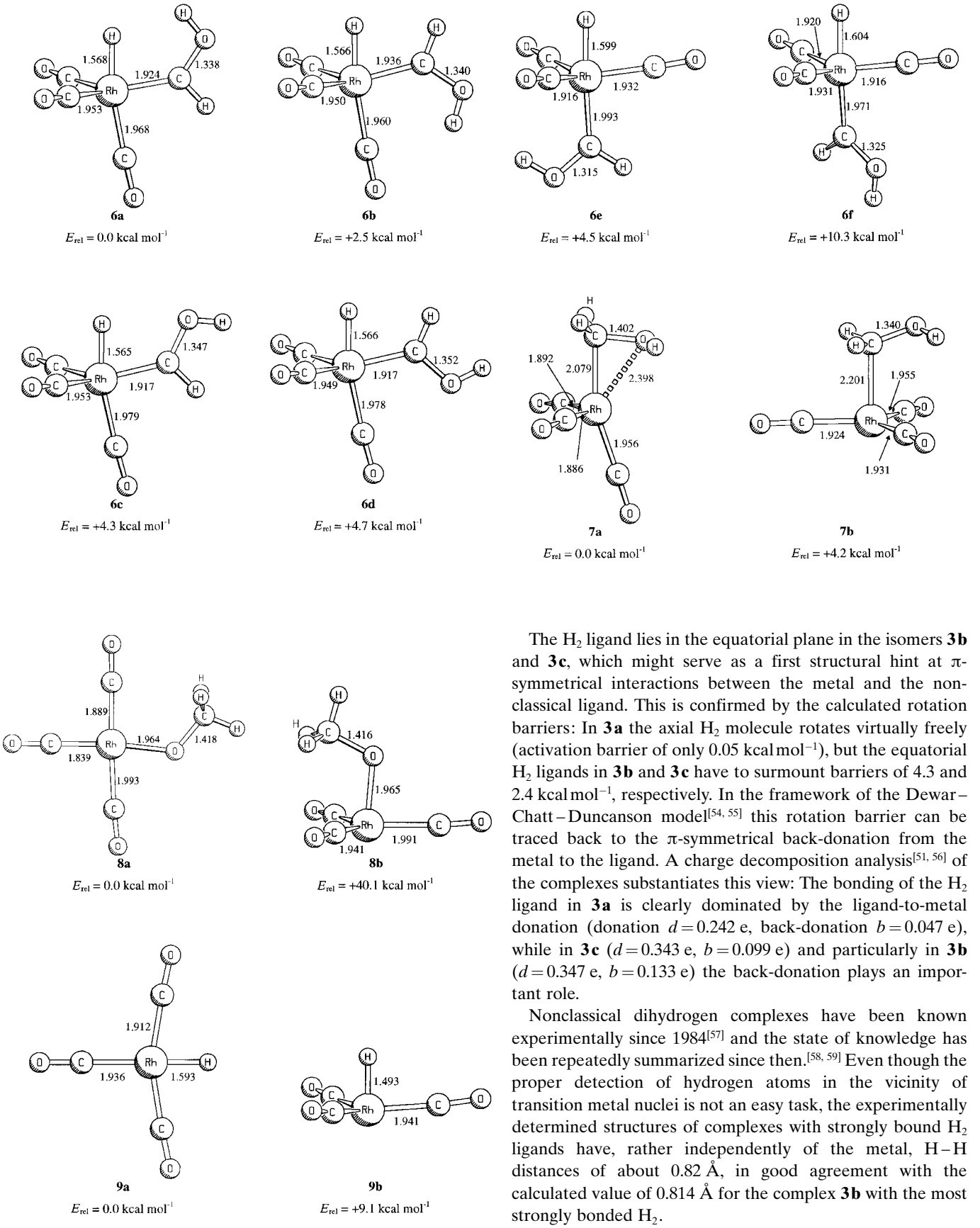

Figure 2. Optimized geometries (MP2/II) of the energy-minimum conformations for the individual intermediates of the postulated catalytic mechanism. Bond lengths in Å. Energies are given relative to the most stable conformer for each intermediate (isomer a).

The H_2 ligand lies in the equatorial plane in the isomers **3b** and **3c**, which might serve as a first structural hint at π-symmetrical interactions between the metal and the nonclassical ligand. This is confirmed by the calculated rotation barriers: In **3a** the axial H_2 molecule rotates virtually freely (activation barrier of only 0.05 kcal mol^{-1}), but the equatorial H_2 ligands in **3b** and **3c** have to surmount barriers of 4.3 and 2.4 kcal mol^{-1}, respectively. In the framework of the Dewar–Chatt–Duncanson model[54, 55] this rotation barrier can be traced back to the π-symmetrical back-donation from the metal to the ligand. A charge decomposition analysis[51, 56] of the complexes substantiates this view: The bonding of the H_2 ligand in **3a** is clearly dominated by the ligand-to-metal donation (donation $d = 0.242$ e, back-donation $b = 0.047$ e), while in **3c** ($d = 0.343$ e, $b = 0.099$ e) and particularly in **3b** ($d = 0.347$ e, $b = 0.133$ e) the back-donation plays an important role.

Nonclassical dihydrogen complexes have been known experimentally since 1984[57] and the state of knowledge has been repeatedly summarized since then.[58, 59] Even though the proper detection of hydrogen atoms in the vicinity of transition metal nuclei is not an easy task, the experimentally determined structures of complexes with strongly bound H_2 ligands have, rather independently of the metal, H–H distances of about 0.82 Å, in good agreement with the calculated value of 0.814 Å for the complex **3b** with the most strongly bonded H_2.

[(HCO)Rh(CO)$_3$H$_2$] (4): Oxidative addition of the coordinated dihydrogen ligand in **3** leads to the classical dihydrido

complex **4**. One can think of 13 different ways of arranging the six ligands around the rhodium centre, if rotations of the formyl group are taken into account. Geometry optimizations starting from these 13 structures (see supporting information) lead to the six minima **4a–f** on the potential energy surface depicted in Figure 2.

The C_1 symmetrical isomer **4a** is energetically more stable than the other five conformers by more than 13 kcal mol^{-1}. In this way, the most stable dihydrido complex **4a** is 3.2 kcal mol^{-1} lower in energy than the nonclassical dihydrogen complex **3b**. The two H atoms of **4a** are *cis* to each other with Rh–H bond lengths of 1.583 Å and 1.603 Å, which are only slightly longer than in the five-coordinate starting catalyst [HRh(CO)$_4$] (1.566 Å). The formyl group is eclipsed with one of the carbonyl ligands and an H atom, but the barrier for its rotation amounts to only 0.6 kcal mol^{-1}. The pseudooctahedral structure is slightly distorted, because the formyl ligand and the *trans*-CO group are bent towards the sterically less demanding hydride ligands.

Two of the remaining five energy-minimum structures have their hydrogen atoms positioned *trans* to each other (**4b** and **4c**), while the other three isomers (**4d–f**) have *cis* hydride ligands, but still a meridional arrangement of the carbonyl groups. **4b** and **4c** as well as **4d–f** differ just by rotation of the formyl ligand. It is notable that the Rh–H distance increases to 1.639 Å–1.646 Å when the hydride ligand is *trans* to another hydride ligand or to the formyl group. The H atom as a pure donor ligand can obviously form stronger bonds to the metal if it is in the *trans* position to a back-donating carbonyl group than if it has to compete with another pure donor ligand in the *trans* position.

In spite of the large number of energy-minimum structures for the dihydrido complex **4**, in the catalytic mechanism most probably only the isomer **4a** will play an important role. It is more stable than the other isomers by more than 13 kcal mol^{-1}, and if one compares its structure with the geometries of the dihydrogen complexes **3b** and **3c** one can anticipate that its formation by oxidative addition of the H_2 ligand should not be a kinetic problem either. This assumption will be confirmed in the subsequent sections.

[HRh(CO)$_3$(CH$_2$O)] (5): The formaldehyde ligand can adopt three fundamental modes of coordination in transition metal complexes: *End-on* coordination by a lone pair of the oxygen atom, *side-on* coordination through the C–O π orbital, or oxidative addition of the CH_2O molecule to form a metallaoxacyclopropane. Taking into account these three modes of coordination, 27 starting structures (see supporting information) have been considered in the geometry optimizations of the fifth intermediate of the catalytic mechanism in Figure 1, **5**. Starting from these 27 structures, only five energy-minimum structures are found (**5a–e**, Figure 2). All of them can be derived from a trigonal bipyramid; in two isomers the formaldehyde ligand is coordinated side-on, in the other three isomers it is coordinated in an end-on fashion.

The structure **5a** is the clearly favoured isomer. It is more stable than the alternative conformations by 3.8–5.4 kcal mol^{-1}. The hydride ligand occupies an axial position in the trigonal bipyramidal coordination sphere around the rhodium centre. The formaldehyde ligand is side-on coordinated in the equatorial plane. The C–O bond length is only slightly elongated from 1.221 Å in the free molecule to 1.306 Å in the complex; it still mainly has the character of a double bond (typical C–O single bond lengths amount to 1.43 Å). Besides, the coordinated formaldehyde molecule is only slightly distorted from planarity. The structure of **5a** thus points clearly to a donor–acceptor type of bonding between the formaldehyde ligand and the metal fragment, as has been substantiated for a number of CH_2O complexes of low-valent transition metals.[60–63] The charge decomposition analysis confirms this supposition: The bonding can be understood in the framework of the Dewar–Chatt–Duncanson model with ligand-to-metal donation ($d = 0.267$ e) being in the same order of magnitude as metal-to-ligand back-donation ($b = 0.206$ e). This π-symmetrical back-donation can also explain the large activation barrier of 7.8 kcal mol^{-1} for the rotation of the formaldehyde ligand.

The remaining four minimum structures of [HRh(CO)$_3$(CH$_2$O)] are energetically very similar to each other. The isomers **5b** and **5d** have the formaldehyde ligand and the hydride ligand in *trans* diaxial positions. They differ only in the coordination of the CH_2O molecule: In **5b** it is end-on coordinated, while it adopts side-on coordination in **5d**. Thus, the two principal modes of coordination of the formaldehyde ligand can be found side by side as minima on the potential energy surface. As in **5a**, in the isomers **5c** and **5e** the H atom occupies an axial position and the CH_2O ligand an equatorial position. However, here the formaldehyde molecule is end-on coordinated and correspondingly the C–O bond length is only 1.228 Å or 1.229 Å, respectively, as compared to 1.306 Å in **5a**.

Versluis and Ziegler have investigated the structure of the related complex [HCo(CO)$_3$(CH$_2$O)] at the local density-functional level using the Hartree–Fock–Slater method.[34] They carried out geometry optimizations in C_S symmetry, but did not calculate the energy Hessian to characterize their stationary points. Besides, they only looked at trigonal bipyramidal structures with side-on coordinated formaldehyde. Since they did not account for geometries of the type **5a**, the lowest energy structures they found had the CH_2O ligand in an equatorial position, but not lying in the equatorial plane. Structures of that kind could be shown in the present study to be transition states of formaldehyde rotation starting from **5a**. This clearly demonstrates the necessity of a frequency characterization of the stationary points found, in particular when symmetry is used during the geometry optimizations.

Altogether we have detected five energy-minimum structures for the fifth stage of the catalytic mechanism in Figure 1. However, the side-on complex **5a** is energetically favoured by 3.8–5.4 kcal mol^{-1}. As will be shown in the next section, its structure also fits best into the reaction sequence. It should thus be the only isomer of **5** of importance for the catalytic mechanism, provided it is kinetically accessible. This will be investigated in the third part of the discussion (Part 3).

[HRh(CO)$_3$(CHOH)] (6): As an alternative to the formaldehyde complex **5**, the formyl intermediate **4** can rearrange to the hydroxycarbene complex **6** (Figure 1). Starting from

0947-6539/98/0403-0528 $ 17.50+.50/0 *Chem. Eur. J.* **1998**, *4*, No. 3

26 isomeric structures, the geometry optimizations led to six minima on the potential energy surface (**6a–f**, Figure 2). The structures **6a–d** can be derived from a trigonal bipyramid with axial hydride and equatorial hydroxycarbene ligand. It is striking that the carbene group is in all cases perpendicular to the equatorial plane. In this way, back-donation from the filled rhodium d orbital to the empty p_π orbital at the carbene C atom is possible. The charge decomposition analysis for the most stable isomer **6a** confirms this bonding picture: The CHOH group can be understood as a donor–acceptor ligand with rather similar values for donation ($d = 0.409$ e) and back-donation ($b = 0.351$ e). The back-donation leads to a substantial degree of double-bond character for the metal–carbene bond, which explains the short Rh–C distances of 1.917 Å–1.936 Å. The complexes **6a–d** just differ by rotation of the hydroxycarbene ligand around the Rh–C bond and by rotation of the hydroxy group around the C–O bond. The competition of the filled d orbital at Rh and the filled p orbital at O for the unoccupied carbene C-p_π orbital is nicely reflected by the structures: The shorter the Rh–C bond, the longer the C–O bond, and vice versa.

The remaining two isomers **6e** and **6f** have a *trans* diaxial arrangement of the hydride and the hydroxycarbene ligand. The C_S symmetrical structure **6e** is clearly more stable than the unsymmetrical isomer **6f**; it seems to have found a conformational niche with the hydroxy group in a staggered position between two carbonyl ligands. This is also reflected by the activation barrier for the rotation of the carbene ligand that amounts to 6.7 kcal mol^{-1} in **6e**, as compared to only 0.9 kcal mol^{-1} in **6f**. The rhodium–carbene bond is longer than in **6a–d**, with a corresponding shortening of the carbene C–O bond.

Hydroxycarbene complexes are frequently discussed as intermediates in the catalytic hydrogenation of carbon monoxide, and we could in fact detect them as minima on the potential energy surface. However, as will be discussed in the following section, the complexes **6a–d** are more than 13 kcal mol^{-1} less stable than the alternative formaldehyde complex **5a**. If there are no kinetic reasons excluding the formaldehyde pathway, *the hydroxycarbene complexes should thus play no role in the mechanism of the catalysis.*

[Rh(CO)$_3$(CH$_2$OH)] (7): The formaldehyde complex **5** or the hydroxycarbene complex **6** can rearrange to the hydroxymethyl complex **7** as the seventh stage of the catalytic mechanism (Figure 1). If one takes into account the fact that the H atom of the hydroxy group can be *syn* or *anti* to the rhodium centre, one has to consider four planar isomers and 26 isomers derived from a trigonal bipyramid with one empty coordination site. In spite of this large number of 30 starting structures, the systematic geometry optimizations yielded just two minima on the potential energy surface, **7a** and **7b** (Figure 2).

The more stable isomer **7a** has the structure of a trigonal bipyramid with an axial hydroxymethyl ligand and an empty coordination site in the equatorial position. The OH group is rotated in such a way that one of the lone pairs at oxygen can interact with the rhodium centre. The importance of this stabilizing coordination is reflected by the high activation barrier for the rotation of the hydroxy group: The transition state with the hydrogen atom *anti* to Rh lies 7.3 kcal mol^{-1} above **7a**, and the corresponding *syn* transition state, where no interaction between the lone pairs at oxygen and the rhodium centre is possible any more, is 9.0 kcal mol^{-1} less stable than **7a**.

The second energy-minimum structure **7b** is less favoured than **7a** by only 4.2 kcal mol^{-1}. It can also be derived from a trigonal bipyramid with axial hydroxymethyl group, but here the empty coordination site is in the axial position. Consequently, the μ^2-coordination of the CH_2OH group has to be given up in **7b**, resulting in a lengthening of the Rh–C bond and a corresponding shortening of the C–O distance. The hydroxy group is rotated in the same way as in **7a**, minimizing the repulsion with the equatorial carbonyl ligands. The rotation barriers for the OH group indicate that this arrangement is a very stable local minimum; they amount to 5.8 kcal mol^{-1} for the transition state with the hydrogen atom *syn* to the rhodium centre and to as much as 10.5 kcal mol^{-1} for the *anti* rotation.

It should be noted that the calculated energy-minimum structures for the formyl complex [(HCO)Rh(CO)$_3$] (**2a** and **2b**) and for the hydroxymethyl complex [(CH$_2$OH)Rh(CO)$_3$] (**7a** and **7b**) are surprisingly similar. In the formyl case, the μ^2-complex **2b** is slightly less stable than the alternative isomer **2a**, whereas in the hydroxymethyl case the μ^2-isomer **7a** is slightly favoured. However, the geometries of **2b** and **7a** and the geometries of **2a** and **7b** clearly correspond to each other, as could have been expected with regard to the chemical similarity of the ligands CHO and CH_2OH.

Versluis and Ziegler have investigated the structure of the related complex [Co(CO)$_3$(CH$_2$OH)] in their DFT study on the insertion of CH_2O into the Co–H bond.[34] However, they restricted their search to selected C_S symmetrical structures that fitted well into the mechanism discussed, and they did not characterize the stationary points by calculating the energy Hessian. In this way, they could not find unsymmetrical energy minima of the type **7a** or **7b**. All the structures presented by Versluis and Ziegler have been proven to be saddle points for the corresponding Rh complexes in the present study. This observation makes Ziegler's results dubious and presents further justification for the systematic and unbiased approach chosen in the present work.

[Rh(CO)$_3$(OCH$_3$)] (8): In addition to the hydroxymethyl complex **7**, a methoxy complex (**8**) is discussed as an intermediate in the catalytic hydrogenation of carbon monoxide. Systematic geometry optimizations starting from 32 theoretically reasonable structures yielded only two minima on the potential energy surface, **8a** and **8b** (Figure 2). The quadratic planar complex **8a** is more stable than the second minimum **8b** by 40.1 kcal mol^{-1}. This is in contrast to the remaining four-coordinate complexes of the type Rh(CO)$_3$X investigated so far: For the formyl compound (X = CHO, **2**) and the hydroxymethyl compound (X = CH_2OH, **7**) only structures derived from a trigonal bipyramid were found. Obviously, the methoxy ligand is electronegative enough to justify a description of [Rh(CO)$_3$(OCH$_3$)] as an ionic complex

between a $Rh^{I}(d^{8})$ fragment and a methanolate ion, for which the ligand-field theory predicts a quadratic planar structure.

In **8a** the methyl group is staggered to the neighbouring carbonyl ligand, but the barrier for its rotation amounts to only 0.7 kcal mol^{-1}. Rotation of the whole methoxy group around the Rh – O axis costs 2.7 kcal mol^{-1}. A pronounced *trans* influence can be noticed in the structure. The CO ligand standing *trans* to the strong donor $CH_3O^-$is tightly bound to the metal centre (1.839 Å). In contrast to that, the carbonyl group towards which the lone pairs of the methoxy oxygen point is at a remarkably long distance from Rh (1.993 Å).

The second energy minimum **8b** certainly plays no role in the catalytic mechanism. Its structure is derived from a trigonal bipyramid with an axial methoxy group and an empty coordination site *trans* to CH_3O, also in the axial position. The methoxy ligand is staggered between two of the equatorial carbonyl groups, but it can rotate with a barrier of only 0.9 kcal mol^{-1}. In contrast, the barrier for rotation of the methyl group amounts to 3.4 kcal mol^{-1}, because in the transition state one of the hydrogen atoms gets very near to the equatorial carbonyls.

[HRh(CO)$_3$] (9): Dissociation of a CH_2O molecule from the formyl complex **4** or from the formaldehyde complex **5** leads to the coordinatively unsaturated species $[HRh(CO)_3]$. It can add a molecule of CO, and in this way the active catalyst $[HRh(CO)_4]$ is rebuilt and the catalytic cycle is closed. For the geometry optimization of $[HRh(CO)_3]$ one quadratic planar structure, four structures derived from a trigonal bipyramid and one distorted pseudotetrahedral structure were considered. Two energy-minimum isomers could be detected (**9a** and **9b**, Figure 2). The quadratic planar form **9a** is more stable than the C_{3v} symmetrical isomer **9b** by 9.1 kcal mol^{-1}. In this respect, $[HRh(CO)_3]$ is similar to the methoxy complex **8**, in which the preference for the planar form is still more pronounced (40.1 kcal mol^{-1}).

Experimentally, $[HRh(CO)_3]$ has not yet been observed.[64] However, in a recent theoretical study R. Schmid et al. determined its structure using density-functional theory.[65] These authors obtained very similar bond lengths as in **9a**, but their calculated structure slightly departs from planarity. The difference to the results of the present work might be traced back to the rather crude local density functional used or to the complete neglect of relativistic effects in the DFT study.

2. Thermodynamic reaction mechanism: The systematic geometry optimizations for the postulated intermediates of the catalytic hydrogenation of carbon monoxide yielded a rather moderate number of energy-minimum structures (Figure 2). The question is now: How do the geometries of the various stages fit into the mechanism and which energetic profile results for the reaction sequence? Figure 3 summarizes the results of the geometry optimizations. The structures of

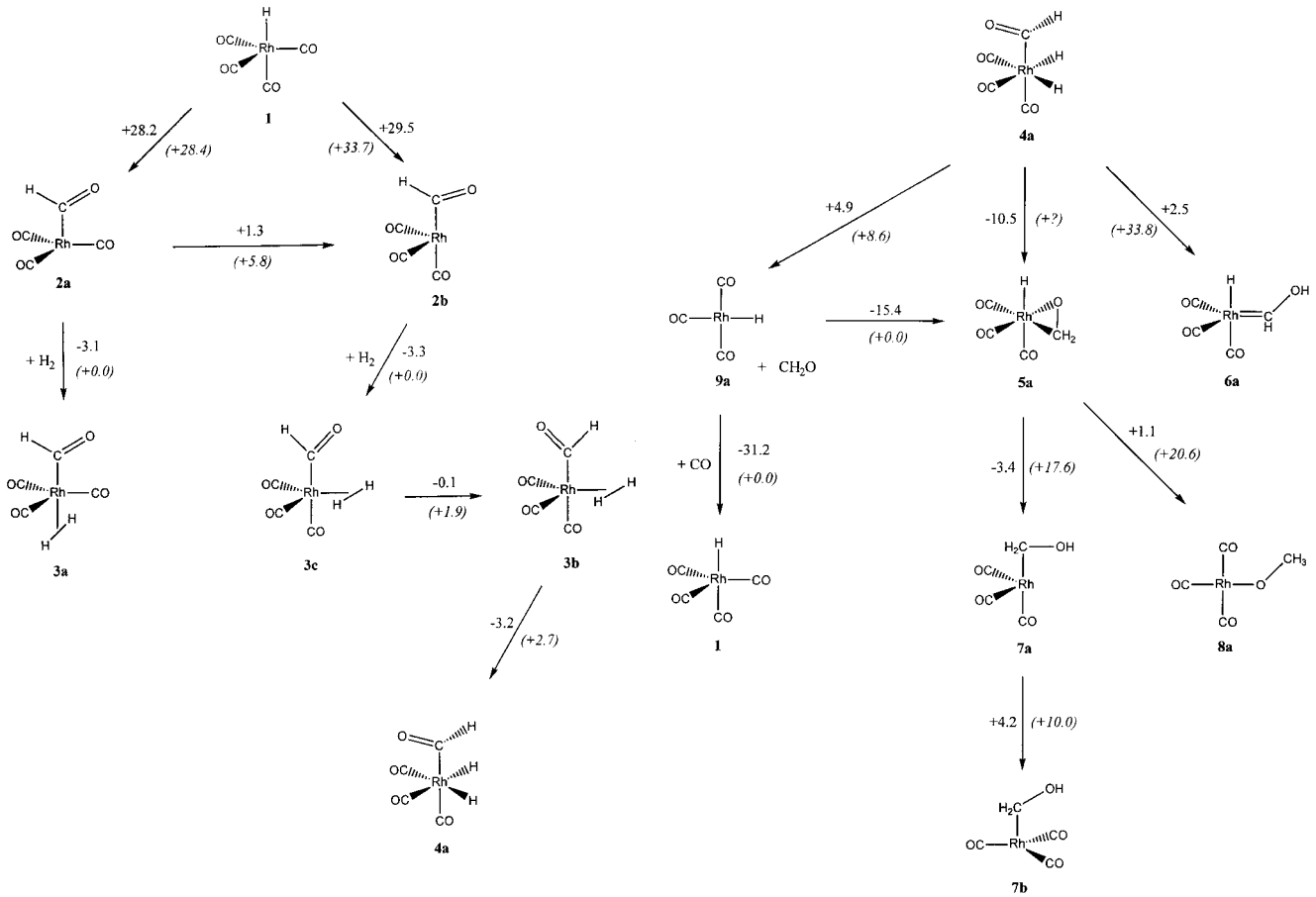

Figure 3. Calculated reaction mechanism (MP2/II) for the $[HRh(CO)_4]$-catalyzed hydrogenation of CO. Reaction energies and activation energies (in parentheses) in kJ mol^{-1}.

0947-6539/98/0403-0530 $ 17.50+.50/0 *Chem. Eur. J.* **1998**, *4*, No. 3

the relevant isomers are shown schematically and are interconnected by arrows. The individual reaction energies are given without correction for the zero-point vibrational energy. The values in parentheses indicate activation energies for the reaction steps and should be ignored at this stage. In the following, we will briefly discuss the calculated reaction sequence step by step.

For the starting catalyst $[HRh(CO)_4]$ (**1**) only the C_{3v}-symmetrical minimum on the potential energy surface was found. Hydride migration or CO insertion may lead to the formyl complexes **2a** or **2b**, which differ energetically by only 1.3 kcal mol^{-1}. However, their formation from **1** is endothermic by 28.2 and 29.5 kcal mol^{-1}, respectively. This result is in qualitative agreement with chemical experience: A hydride migration to a carbonyl group has never been observed experimentally, while the back-reaction of a formyl complex to a hydridocarbonyl complex is rather common.[2, 18, 20] Nevertheless, formyl complexes can certainly play a role as transitory intermediates in catalytic reactions. The reaction energy for their formation from hydridocarbonyl species was estimated from bond energies to be of the order of 30–40 kcal mol^{-1},[20] which is in good agreement with the calculated results.

For the third stage of the reaction, the complex $[(HCO)Rh(CO)_3(H_2)]$, the systematic geometry optimizations yielded three energetically very similar minima **3a–c**. If one compares the calculated structures, one notices immediately that both **3a** and **3c** should be easily accessible from **2a** and **2b**, respectively, by simple addition of an H_2 molecule to the empty coordination site at rhodium. Furthermore, **3b** can be obtained from **3c** by simple rotation of the formyl group. The reaction energy for the H_2 addition is slightly exothermic by 3.1 and 3.3 kcal mol^{-1}, respectively. The nonclassical dihydrogen complexes **3a–c** thus fit well into the catalytic mechanism from a structural and from an energetic point of view; they are plausible intermediates of the catalysis.

Up to this stage all calculated minimum structures are thermodynamically accessible and **3a** is more favourable than **3b** and **3c** by only 1 kcal mol^{-1}. For the fourth stage of the reaction, the dihydridoformyl complex $[(HCO)Rh(CO)_3H_2]$, six energy minima were found, but the isomer **4a** is the most stable by more than 13 kcal mol^{-1} (Figure 2). However, does **4a** also match structurally with its mechanistic precursors **3a–c**? A look at the calculated geometries shows that **4a** can be obtained from **3b** by simple oxidative addition of the H_2 ligand and a slight rotation of the formyl group. This reaction is exothermic by 3.2 kcal mol^{-1}. Thus, even though **3a** is the slightly preferred isomer of the dihydrogen complexes, it seems to be a thermodynamic impasse, because a direct reaction to the most favourable dihydrido complex **4a** is mechanistically not possible. However, **3b** should easily react to **4a** and the equilibrium of the dihydrogen complexes can be supposed to shift towards **3b**. Of course, this mechanism depends heavily on the activation energies of the individual reaction steps, which will be discussed in the following section. In any case, the most stable dihydrido complex **4a** seems to be mechanistically easily accessible, and we have to consider only one isomer of this central intermediate of the catalysis.

The dihydridoformyl complex **4a** can either rearrange to the formaldehyde complex **5** by hydride migration to the formyl carbon atom or to the hydroxycarbene complex **6** by H migration to the formyl oxygen atom. For $[HRh(CO)_3(CH_2O)]$ (**5**) five minima on the potential energy surface were found (Figure 2). The energetically most stable isomer **5a** also fits best into the mechanistic sequence: Complexes **5c** and **5e** with end-on coordinated formaldehyde can be obtained from **4a** only after rearrangement, while the *trans* orientation of CH_2O and the hydride ligand in **5b** and **5d** renders subsequent reactions very difficult. The formation of **5a** from **4a** is strongly exothermic by 10.5 kcal mol^{-1}.

For the hydroxycarbene intermediate $[HRh(CO)_3(CHOH)]$ the most stable isomers **6a** and **6b** should also be the most easily accessible isomers from a structural point of view. In the complexes **6c** and **6d** the hydroxy H atom is in *anti* position to the Rh centre to which it bonds in the precursor **4a**, and in the isomers **6e** and **6f** the carbene and the hydride ligand are in *trans* arrangement preventing subsequent reactions without prior rearrangement. However, even the formation of **6a** from **4a** is endothermic by 2.5 kcal mol^{-1} and thus thermodynamically less favourable than the competing exothermic formation of **5a** by 13 kcal mol^{-1}. From a thermodynamic point of view the hydroxycarbene complexes should thus play no role in the catalytic mechanism. Nevertheless their participation can only be safely excluded when the activation barriers of the competing reactions are taken into account. It is still possible that the formation of **5a** loses out against the formation of **6a** on kinetic grounds.

By a further hydride migration the intermediate **5a** can react to give either the hydroxymethyl complex **7** or the methoxy complex **8**. For $[Rh(CO)_3(CH_2OH)]$ (**7**) the systematic geometry optimizations yielded two minima on the potential energy surface (Figure 2). The structure of the more stable isomer **7a** indicates that it should be directly accessible from **5a**. The rearrangement is exothermic by 3.4 kcal mol^{-1}. The alternative isomer **7b** is 4.2 kcal mol^{-1} less stable. It can be obtained from **7a** by moving the axial carbonyl ligand into the equatorial plane and simultaneously rotating the hydroxymethyl group. In this way, both conformers of **7** are structurally and energetically plausible intermediates of the catalytic mechanism. By adding a molecule of H_2 or CO they can continue the reaction and eventually lead to the formation of methanol and other products containing a CH_2OH group.

The alternative reaction of **5a** to the only relevant methoxy complex **8a** is endothermic by 1.1 kcal mol^{-1} (Figure 3). The formation of **8a** is thus thermodynamically only slightly less favourable than the competing formation of **7a**. This result can explain the frequently observed occurrence of methoxy products like methyl formate and methyl acetate in the Rh-catalyzed hydrogenation of carbon monoxide. The kinetic aspects of the selectivity between hydroxymethyl and methoxy products are treated in the subsequent section.

The transitory occurrence of formaldehyde in the CO hydrogenation reaction might be explained by the loss of the CH_2O ligand from **5a** or by direct formation of CH_2O from the formyl complex **4a**. Both reactions are endothermic (Figure 3), but the formation from **4a** (+4.9 kcal mol^{-1}) is

clearly more favourable than the dissociation from **5a** (+15.4 kcal mol^{-1}). It should be noted that the reactions are expected to be less endothermic in solution, because the coordinatively unsaturated complex [HRh(CO)$_3$] (**9a**) arising can be stabilized by interaction with solvent molecules. An assessment of such solvent effects is given in the final discussion of the overall reaction profile (section 4). The planar complex **9a** can now add a formaldehyde molecule and (re)form complex **5a** in a strongly exothermic reaction (−15.4 kcal mol^{-1}). Alternatively, it can add a molecule of carbon monoxide and close the catalytic cycle by rebuilding the active catalyst [HRh(CO)$_4$] (**1**). The latter reaction is clearly preferred thermodynamically (−31.2 kcal mol^{-1}). However, which reaction actually takes place also depends on the individual activation barriers and on the relative local concentrations of CO and CH_2O.

The summary of the thermodynamic reaction mechanism in Figure 3 shows that the calculations yield a rather smooth reaction profile, even though in the geometry optimizations all theoretically reasonable structures were taken into account, not just those which fit well into the postulated mechanism anyway. For all intermediates, the most stable isomers fit best into the reaction mechanism from a structural point of view. In spite of the huge number of starting structures, the mechanism of the catalysis remains rather simple, because for most stages one isomer clearly dominates. Besides this, neither thermodynamic traps nor energetically inaccessible isomers are found. However, up to this stage the mechanism is only characterized by the structures and energies of the stable intermediates. The inclusion of kinetic aspects might change this picture considerably. Therefore, in the next section we will discuss the transition states and activation barriers for the individual reaction steps.

3. Transition states of the catalytic mechanism: All transition state searches were performed in C_1 symmetry. In cases where several reaction pathways are theoretically possible (e.g., two possible hydrogen atoms that can migrate, yielding three possible relative arrangements of the remaining ligands), each route was investigated individually. Of course, all transition states described were proven to be first-order saddle points on the potential energy surface by explicit calculation of the energy Hessian. The transition states were further characterized by the eigenvector corresponding to the negative eigenvalue of the Hessian and by calculation of the intrinsic reaction coordinate (IRC) connecting them with the corresponding energy-minimum structures. Figure 4 summarizes the calculated transition states giving the profiles of the individual reaction steps and the energies relative to the respective reactant.

TS1*: *1*→*2a: The formation of the formyl complex **2a** from the starting catalyst [HRh(CO)$_4$] (**1**) is strongly endothermic (28.2 kcal mol^{-1}). However, Figure 4a shows that virtually no additional barrier has to be overcome: The transition state **TS1** is less stable than the product by only 0.2 kcal mol^{-1}. In accordance with Hammond's postulate[66] **TS1** is a late transition state and is structurally very similar to the product of the reaction. It is clear from the reaction profile that the formation of the formyl group results from hydride migration to the carbonyl ligand, and not from CO insertion into the Rh–H bond.

TS2*: *1*→*2b: The formation of the alternative formyl complex **2b** from the active catalyst **1** is a slightly more complicated process. As described above, the C_{3v}-symmetrical minimum structure of [HRh(CO)$_4$] (**1**) can perform a degenerate Berry pseudorotation passing a C_{2v}-symmetrical transition state **1**** corresponding to a trigonal bipyramidal structure with an equatorial hydride ligand (Figure 4b). The barrier for this rotation amounts to 13.4 kcal mol^{-1}. The C_{2v}-symmetrical isomer **1*** can now be transformed to the formyl complex **2b** by hydride migration (Figure 4c). The transition state **TS2** for this reaction is also a first-order saddle point on the potential energy surface. Of course, this somehow unexpected reaction course had to be confirmed by calculation of the intrinsic reaction coordinate connecting the stationary points. The overall barrier for the transformation **1**→**2b** amounts to 33.7 kcal mol^{-1}; in the transition state **TS2** the migration of the hydrogen atom has already largely taken place.

TS3*: *2a*→*2b: The two calculated energy-minimum structures of [(HCO)Rh(CO)$_3$], **2a** and **2b**, are energetically and structurally very similar. In both isomers the formyl group lies in the symmetry plane of the molecule. However, Figure 4d indicates that the transformation of **2a** to **2b** is not as simple as might have been expected from the geometries of the minima. In the transition state **TS3** the symmetry of the molecule is lost: The formyl group is slightly rotated out of the former symmetry plane in order to build up a stabilizing interaction with the rhodium centre even before the carbonyl ligand is completely bent to the axial position. This slight rotation diminishes the activation barrier of the reaction by about 0.5 kcal mol^{-1}. The C_S-symmetrical second-order saddle point that results from rotation of the formyl group into the molecular plane lies 6.3 kcal mol^{-1} above **2a**, compared to 5.8 kcal mol^{-1} for **TS3**.

TS4*: *2a*+H_2→*3a: The calculated structures of the minima **2a** and **3a** indicate that the addition of H_2 to the empty coordination site at Rh in **2a** should be possible without great effort. Indeed, we could not locate any transition state for this exothermic reaction (Figure 4e). Using the reaction coordinate method we could show that the addition really takes place without an activation barrier: Optimization of the remaining degrees of freedom for a set of fixed Rh–H_2 distances yields a monotonous decrease of the energy upon approach of the H_2. It should be noted that the situation is probably changed in solution. The coordinatively unsaturated complex **2a** will be stabilized by coordination of a solvent molecule that has to be displaced by the incoming dihydrogen.

TS5*: *2b*+H_2→*3c: The exothermic formation of **3c** by addition of H_2 to the formyl complex **2b** also takes place without activation barrier (Figure 4f). The reaction coordinate method shows that the H_2 molecule approaches from slightly below the equatorial plane so that the stabilizing

0947-6539/98/0403-0532 $ 17.50+.50/0 *Chem. Eur. J.* **1998**, *4*, No. 3

interaction between the formyl oxygen atom and the rhodium centre can be preserved until the Rh–H_2 interaction is built up. In this way, an energy maximum along the reaction path is bypassed. Again, in solution a small barrier might occur if the incoming H_2 molecule has to replace a solvent molecule.

TS6*: *3c*→*3b: The two isomers **3b** and **3c** of [(HCO)Rh-$(CO)_3(H_2)$] are energetically very similar (0.1 kcal mol^{-1}) and differ structurally only by the rotation of the formyl group. As expected, they are transformed into one another with a small activation barrier of only 1.9 kcal mol^{-1} (Figure 4g). In the transition state **TS6** the rotation is exactly halfway complete; the formyl group is parallel to the coordinated H_2 ligand.

TS7*: *3b*→*4a: The transformation of the dihydrogen complex **3b** to the dihydrido complex **4a** is exothermic by 3.2 kcal mol^{-1}. The breaking of the H–H bond is accompanied by a slight rotation of the formyl group. Figure 4h shows that the oxidative addition of the dihydrogen ligand requires only a moderate activation energy of 2.7 kcal mol^{-1}. In the transition state **TS7** the rotation of the formyl ligand has already begun and the symmetry of the molecule is lost. The Rh–H bonds are already shortened to 1.640 Å and 1.651 Å. However, the H–H distance of only 1.110 Å indicates that in **TS7** the interaction between the two hydrogen atoms is still preserved.

TS8*: *4a*→*5a: The reaction of the dihydridoformyl complex **4a** to the formaldehyde complex **5a** is highly exothermic, with a reaction energy of -10.5 kcal mol^{-1}. The migration of a hydrogen atom is accompanied by the build-up of an interaction between the oxygen atom of the forming CH_2O ligand and the rhodium centre (Figure 4i). Since both hydride ligands can migrate, the search for a transition state has to consider two separate reaction pathways. However, all attempts to locate a transition state connecting **4a** and **5a** failed. In all cases a dissociation of the formaldehyde molecule from the metal fragment was observed. Likewise, no transition state between **4a** and the less favourable isomers of **5** (Figure 2) could be found, despite careful search. The forming CH_2O molecule constantly dissociated from the complex as soon as one of the hydride ligands approached the formyl carbon atom. The direct formation of **5a** from the formyl complex **4a** can thus fairly safely be excluded. The formation of **5a** by dissociation of CH_2O and subsequent recoordination of the molecule might serve as an alternative reaction pathway.

TS9*: *4a*→*9a* + *CH_2O: For a systematic investigation of the dissociation of formaldehyde from the dihydridoformyl complex **4a** six alternative reaction pathways had to be studied separately, because both hydrogen atoms can migrate and the remaining hydride ligand can be *trans* to one of three carbonyl groups in the planar product **9a**. However, it could be shown that only two reaction paths are actually realized, as was proven by calculating the intrinsic reaction coordinates.

The energetically more favourable reaction pathway passes through transition state **TS9a** (Figure 4j). The activation barrier of the endothermic reaction amounts to a moderate 8.6 kcal mol^{-1}. The front hydrogen atom is migrating, attacking the formyl carbon atom at the C–O π bond, which temporarily becomes slightly longer than in the reactant as well as in the product. The distance between the migrating H atom and the formyl carbon atom is already only 1.357 Å in **TS9a**, even though the Rh–H bond had to lengthen only by 0.1 Å. The still rather short Rh–C bond indicates that **TS9a** is an early transition state.

In the alternative reaction course passing through **TS9b** the other hydrogen atom leaves the rhodium centre (Figure 4k). As in **TS9a**, the carbonyl ligand *trans* to the formyl group follows the migrating hydrogen that again attacks the formyl carbon atom at the C–O π bond. In this case, however, a rotation of the formyl group is necessary to achieve this. This might be the reason for the slightly higher activation barrier of 9.3 kcal mol^{-1}.

TS10*: *9a* + *CH_2O*→*5a: The addition of formaldehyde to the coordinatively unsaturated complex [$HRh(CO)_3$] (**9a**) is highly exothermic, with a reaction energy of -15.4 kcal mol^{-1}. In a first step, the intermediate complex **5c** is formed in which the CH_2O ligand is end-on coordinated (Figure 4l). Even though the formaldehyde C–O bond is lengthened by only 0.008 Å, the coordination energy amounts to 10.5 kcal mol^{-1}. The reaction coordinate method was used to prove that the addition takes place without a barrier. In the second step, the formaldehyde complex **5c** is transformed into its more stable isomer **5a**, which has a side-on coordinated CH_2O ligand (Figure 4m). This rearrangement has a small activation barrier of 2.9 kcal mol^{-1}, but the transition state **TS10** is still more stable than the reactants **9a** + CH_2O by 7.6 kcal mol^{-1}. In agreement with Hammond's postulate the structure of **TS10** is rather similar to the structure of its precursor **5c**.

This reaction pathway could be confirmed by the calculation of the intrinsic reaction coordinate connecting the stationary points. Possibly we have found a mechanistic prototype for the addition of formaldehyde to coordinatively unsaturated transition metal complexes: At large distances, the electrophilic metal starts to interact with the far-reaching free electrons of the formaldehyde oxygen atom, and an end-on complex is formed as first intermediate. Having attracted and prebound the formaldehyde molecule in this way, only a small barrier has to be surmounted for the rearrangement to the more stable side-on complex, which is also better suited for the following metal-mediated reactions at the ligand.

TS11*: *4a*→*6a: The formation of the hydroxycarbene complex **6a** from the formyl complex **4a** was excluded according to thermodynamic criteria because the alternative formation of **5a** is favoured by 13 kcal mol^{-1} (Figure 3). But since we could not find a direct reaction path from **4a** to **5a** (Figure 4i), the hydroxycarbene path might come back into play for kinetic reasons. However, Figure 4n shows that the activation barrier for the migration of a hydrogen atom to the formyl oxygen atom is very high (33.8 kcal mol^{-1}). The calculation of the intrinsic reaction coordinate demonstrates that in a first step the hydroxycarbene complex **6ab*** is formed in an endothermic reaction (+14.9 kcal mol^{-1}). It has the CHOH ligand in the equatorial plane of the trigonal bipyramidal

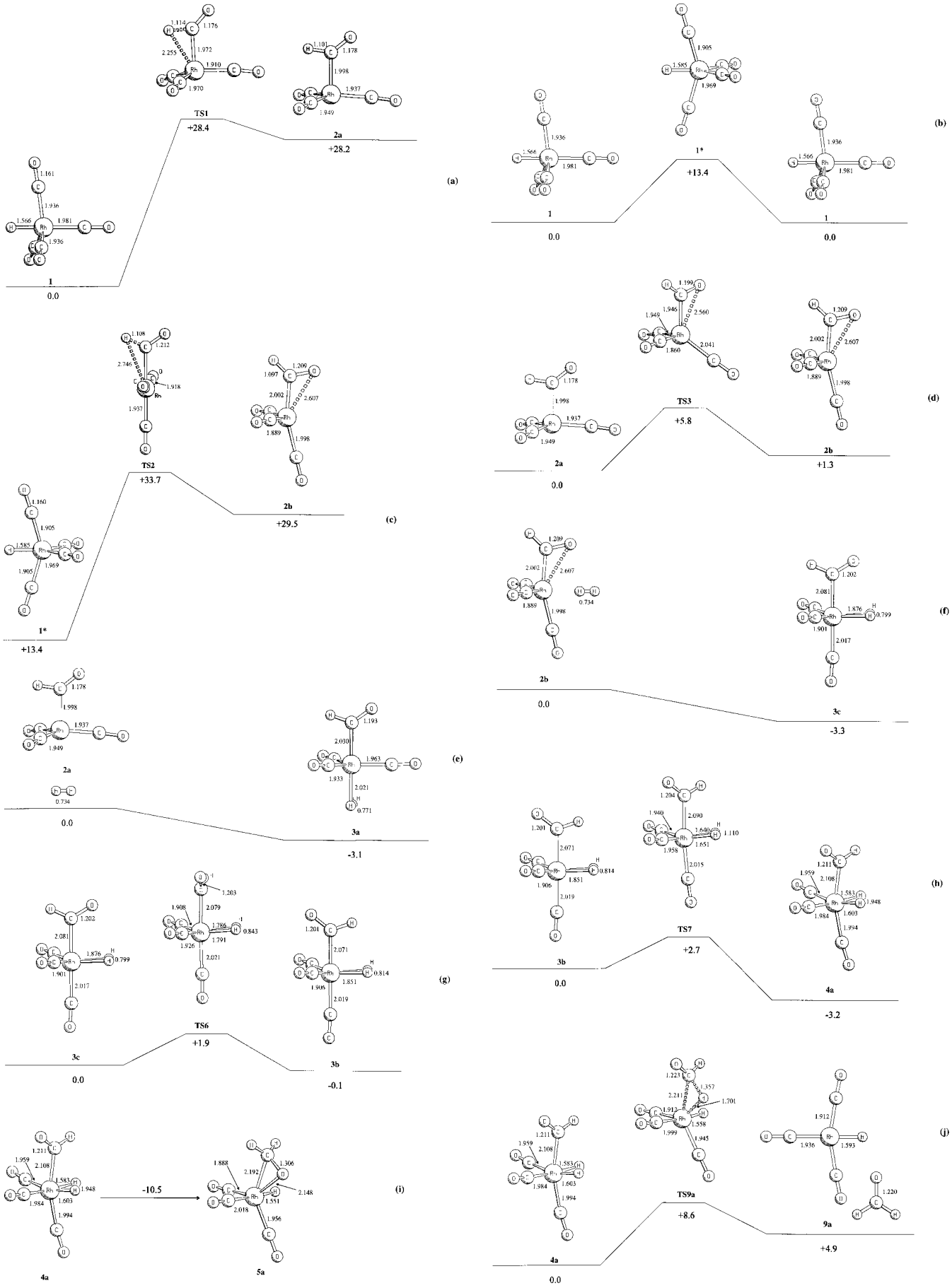

0947-6539/98/0403-0534 $ 17.50+.50/0 *Chem. Eur. J.* **1998**, *4*, No. 3

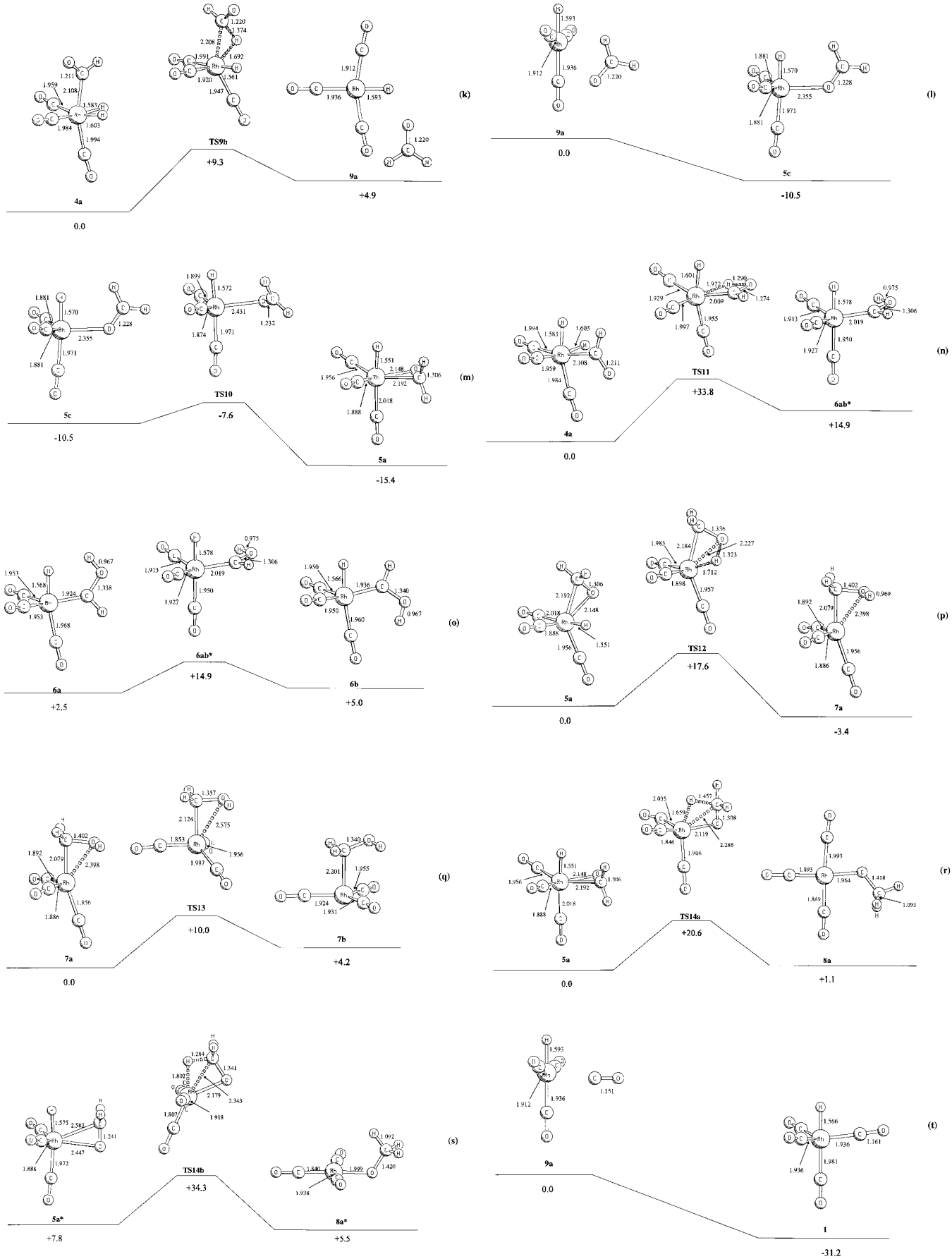

Figure 4. Calculated reaction profile (MP2/II) for the most energetically favoured reaction pathway for the $[HRh(CO)_4]$-catalyzed hydrogenation of CO.

structure. According to the Hammond postulate, the transition state **TS11** is already rather similar to the product: In the course of the reaction the formyl group is first rotated into the equatorial plane prior to migration of the hydrogen atom from Rh to O (Figure 4n).

Structure **6ab*** is a first-order saddle point on the potential energy surface. IRC calculations show that it corresponds to the transition state for the rearrangement between **6a** and **6b** (Figure 4o). The barrier for this transformation is very high (12.4 kcal mol^{-1}). It can be traced back to the planar arrangement of the carbene ligand in **6ab*** that prevents a stabilizing π interaction between the Rh centre and the carbene C atom. Such an interaction results in partial double-bond character for the Rh–C bonds in **6a** and **6b**. Accordingly, the Rh–C bond in **6ab*** is lengthened by about 0.09 Å compared to those in **6a** and **6b**, while the carbene C–O bond is shortened by about 0.03 Å, because the free electrons at oxygen do not have to compete with the rhodium centre for the donation to the carbene C p_π orbital any longer.

The calculations thus show that the H migration to the formyl oxygen atom via **TS11** can lead to either **6a** or **6b**. The formation of **6a** is thermodynamically favoured by 2.5 kcal mol^{-1}. Kinetically, both products are equally probable because they are formed from the same transition state. However, the barrier for the formation of **6a** or **6b** is too high (33.8 kcal mol^{-1}) for the complexes to play a role in the catalytic mechanism; the hydroxycarbene path can also be excluded on kinetic grounds.

The 1,3 hydrogen migration from **4a** to **6a** (or **6b**) is the second example found in this study where two first-order saddle points are directly connected on the potential energy surface without passing through an energy minimum. The first example was the reaction **1**→**2b**. Such situations are theoretically well understood,[67] but examples are very rare.

TS12*: *5a*→*7a: The formaldehyde complex **5a** can transform to the hydroxymethyl complex **7a** in a slightly exothermic reaction (−3.4 kcal mol^{-1}). Although the reaction does not involve big structural changes but only a simple migration of the hydrogen ligand to the formaldehyde oxygen atom (Figure 4p), the activation barrier amounts to 17.6 kcal mol^{-1}. In **TS12** the distance between the migrating H atom and the formaldehyde oxygen atom is already quite short (1.323 Å), but overall the structure of **TS12** is still rather similar to the reactant **5a**: The Rh–H and the Rh–O bond are not much elongated, the Rh–C bond is only slightly shortened and above all the C–O bond with a length of 1.336 Å is more similar to a weakened double bond, as in **5a**, than to the single bond it becomes in the hydroxymethyl complex **7a**.

***TS13*: *7a*→*7b*:** The transformation of the hydroxymethyl complex **7a** to its isomer **7b** is an endothermic reaction (+4.2 kcal mol^{-1}) via transition state **TS13** (Figure 4q). The movement of the axial carbonyl ligand to the equatorial position and the rotation of the hydroxymethyl group take place in a synchronous way. The activation barrier of 10.0 kcal mol^{-1} is higher than expected for the simple rearrangement. It was noted above that the structures of the formyl complexes **2** and the hydroxymethyl complexes **7** are strikingly similar. The same holds for the structures of the transition states **TS3** (**2a**→**2b**) and **TS13** (**7a**→**7b**) (Figure 4d and Figure 4q). In both cases the activation energy of the simple transformation is surprisingly large. It seems that the structures derived from trigonal bipyramids with an axial or equatorial empty coordination site are locally very stable energy minima. They are well-defined geometries in the framework of classical coordination chemistry, and their transformation via less well defined geometries costs a lot of energy.

TS14*: *5a*→*8a: As an alternative to the hydroxymethyl complex **7a**, the formaldehyde complex **5a** can react to the methoxy complex **8a** by migration of the hydrogen ligand to the formaldehyde carbon atom. For this slightly endothermic reaction (+1.1 kcal mol^{-1}) three alternative reaction paths had to be investigated separately, because the forming methoxy group can be *trans* to one of the three carbonyl ligands in the planar product complex **8a**. Figure 4r shows the reaction pathway most favourable by a clear margin: The formaldehyde ligand rotates out of the equatorial plane, and in this way the formaldehyde carbon atom approaches the hydride ligand and pulls it off the rhodium centre. This course of the reaction was verified by an IRC calculation. The transition state **TS14a** is still rather similar to the reactant **5a**. The considerable rearrangement in the ligand sphere requires an activation energy of 20.6 kcal mol^{-1}.

A second possible reaction path leading from **5a** to **8a** was found, but with an overall activation barrier of 34.3 kcal mol^{-1} it is clearly less favourable (Figure 4s). It takes place in a C_S-symmetrical subspace of the potential hypersurface. To reach this subspace, **5a** has first to be transformed to the transition state **5a***, which has the CH_2O ligand perpendicular to the equatorial plane. Starting from **5a*** the formaldehyde molecule can insert into the Rh–H bond, passing through transition state **TS14b**. As a first product the C_S-symmetrical complex **8a*** is formed, which is a second-order saddle point on the potential energy surface. Complex **8a*** can subsequently rearrange to the energy-minimum structure **8a** with an energy gain of 4.4 kcal mol^{-1}. Of course, this complicated reaction sequence had to be confirmed by an IRC calculation. However, in the actual catalytic mechanism this reaction path should play no role, because the reaction via **TS14a** has an activation barrier that is lower by 13.7 kcal mol^{-1}.

TS15*: *9a*+*CO*→*1: The strongly exothermic addition (−31.2 kcal mol^{-1}) of a CO molecule to the coordinatively unsaturated complex [$HRh(CO)_3$] (**9a**) reconstitutes the starting catalyst [$HRh(CO)_4$] (**1**). Partial optimizations with a series of fixed Rh–CO distances unambigously prove that the addition takes place without an activation barrier (Figure 4t). However, as noted above, the situation in solution might be slightly more complicated, because the incoming CO molecule will probably have to displace a solvent molecule which temporarily stabilizes the coordinatively unsaturated intermediate [$HRh(CO)_3$].

4. Calculated mechanism and reaction profile: In the preceding section we have presented the transition states for the

0947-6539/98/0403-0536 $ 17.50+.50/0 *Chem. Eur. J.* **1998**, *4*, No. 3

individual reaction steps of the $[HRh(CO)_4]$-catalyzed hydrogenation of carbon monoxide. We will now summarize these results and discuss the catalytic mechanism of Figure 3 including the information on the activation barriers.

It is clear from Figure 3 that the highly endothermic formation of **2a** from **1** ($+28.2\ kcal\,mol^{-1}$) requires only a small additional barrier of $0.2\ kcal\,mol^{-1}$. In spite of the unusual reaction path, the alternative formation of **2b** also requires an activation of only $4.2\ kcal\,mol^{-1}$. The calculated activation energy of $5.8\ kcal\,mol^{-1}$ for the transformation of **2a** to **2b** makes the direct reaction path from **1** to **2b** and the indirect path via **2a** equally favourable from a kinetic point of view.

The H_2 addition to **2a** and **2b** leading to **3a** and **3c**, respectively, takes place without activation barrier. In this way, the unstable, coordinatively unsaturated formyl complexes **2a** and **2b** can immediately be trapped. The calculated activation energies also explain why the formation of unsaturated formyl complexes by hydride migration from hydridocarbonyl complexes could not be observed experimentally: The back-reaction to the hydridocarbonyl species as well as the stabilizing addition of further ligands is not associated with any substantial kinetic barrier. The formyl complexes should thus be only transient species in the reaction mixture. Possibly, an early approach of the H_2 molecule can support the hydride migration leading to the formyl group, and the complexes **2a** and **2b** do not have to be formed explicitly. This might lower the energy demand of the first step of the reaction.

In the following two slightly exothermic steps the H_2 ligand is first attracted (**3c** → **3b**) and subsequently oxidatively added to the Rh centre (**3b** → **4a**). Both steps have only a small activation energy of 1.9 and $2.7\ kcal\,mol^{-1}$, respectively. The transition-state searches thus show that the thermodynamically most favourable $[(HCO)Rh(CO)_3H_2]$ isomer **4a** is also kinetically easily accessible, confirming the reaction sequence as discussed in section 2.

No reaction path for the direct formation of **5a** from **4a** was found on the potential energy surface. Could the thermodynamically unfavourable hydroxycarbene complexes **6a** and **6b** thus nevertheless play a role in the catalytic mechanism for kinetic reasons? The answer is clearly: No! The activation barrier for the formation of **6a** or **6b** from **4a** is very high ($33.8\ kcal\,mol^{-1}$), while the indirect formation of **5a** by dissociation of formaldehyde from **4a** and subsequent addition of the CH_2O molecule to the formed $[HRh(CO)_3]$ complex **9a** requires an overall activation energy of only $8.6\ kcal\,mol^{-1}$. The hydroxycarbene route can thus also be excluded from a kinetic point of view.

The formaldehyde complex **5a** can transform to the hydroxymethyl complex **7a** or to the methoxy complex **8a**. The activation barriers for the competing reactions are very similar (17.6 and $20.6\ kcal\,mol^{-1}$, respectively). The hydroxymethyl complex should thus be slightly favoured under thermodynamic as well as kinetic conditions. But the energetic difference is so small that both intermediates can be present in the reaction mixture. This is in agreement with the experimental observations: Usually both higher alcohols and methyl esters/methyl ethers are found in the product spectrum,[2] but the main products ethylene glycol, glycolaldehyde and methanol carry a CH_2OH functionality that can be traced back to the hydroxymethyl intermediate.

Formaldehyde can be set free in the reaction course either from the formaldehyde complex **5a** or directly from the formyl complex **4a**. Although the dissociation from **5a** takes place without a barrier, the formation from **4a** remains more favourable even under kinetic conditions, because the corresponding activation barrier of $8.6\ kcal\,mol^{-1}$ lies under the dissociation energy of $15.4\ kcal\,mol^{-1}$ from **5a**. The forming planar complex **9a** can either add CO and reconstitute the active catalyst **1** or add CH_2O and (re)build the intermediate **5a**. Kinetic aspects should play no role, since both reactions require no activation energy. Thermodynamically the CO addition is clearly favoured (-31.2 vs. $-15.4\ kcal\,mol^{-1}$). Nevertheless, formaldehyde is often postulated as an intermediate, but rarely isolated as a product. The thermodynamic effects are thus probably overcompensated by competing influences. Presumably, the local concentration of CH_2O near the reaction centre is enhanced, because the dissociated formaldehyde molecule is not fully removed from the rhodium due to solvent effects. These effects will be further discussed in the following.

Figure 5 shows the complete reaction profile of the most favourable reaction pathway for the $[HRh(CO)_4]$-catalyzed hydrogenation of CO. Although all theoretically reasonable

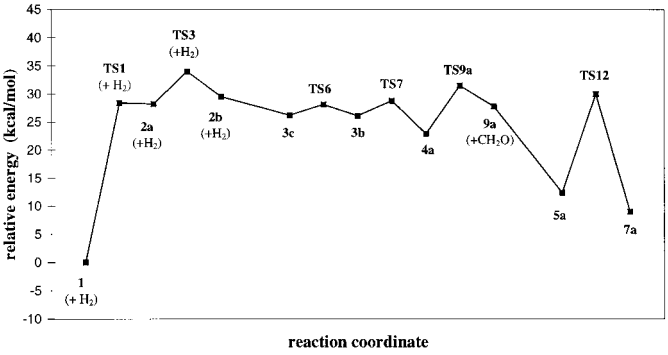

Figure 5. The calculated reaction profile (MP2/II) of the most energetically favoured reaction pathway for the $[HRh(CO)_4]$-catalyzed hydrogenation of CO.

structures were taken into account in the geometry optimizations—not just those which fit well into the mechanism anyway—a rather simple and very smooth profile is obtained, without thermodynamic traps or insurmountable barriers. This presents a strong confirmation of the postulated mechanism. The first step of the catalysis, the formation of the formyl complex $[(HCO)Rh(CO)_3]$ from the starting catalyst $[HRh(CO)_4]$, is the rate-determining step of the whole reaction and thus responsible for the requirement of high temperature and pressure. This result is in agreement with the experimental observation that added CH_2O is immediately reduced or hydroformylated under the conditions of the catalysis, which means that the rate-determining step of the CO hydrogenation must be passed through before a formaldehyde complex is formed.[6, 68] The energy that is required

for the catalysis must thus be provided right at the beginning of the reaction; it is slowly set free in the following slightly exothermic steps.[69]

Of course, the presented calculations refer to reactions in the gas phase in the limit of perfect dilution. A consideration of solvent effects would generally lead to a stabilization of the coordinatively unsaturated intermediates, while the coordinatively saturated complexes would be less influenced. The assessment of solvent effects is rather difficult, because on the one hand a great variety of different solvents is used in practice, among those also very weakly coordinating hydrocarbons, and on the other hand several additives like phosphines and nitrogen bases are employed which can also stabilize the unsaturated intermediates by coordination.

The solvent used could have a substantial influence on the rate-determining step of the catalysis. The unsaturated formyl complex [(HCO)Rh(CO)$_3$] (**2**) should be largely stabilized by solvent coordination, and its formation that is rate-determining in the gas phase could thus be facilitated in solution. On the other hand, the calculations yielded a stabilization energy of only 3 kcal mol^{-1} for the addition of H_2 to the formyl intermediate. If the stabilization of **2** by the solvent is large enough, the displacement of a solvent molecule by the H_2 molecule could thus become the rate-determining step and the dihydrogen complex **3** could become the bottleneck of the reaction.

Another reaction step that can be strongly influenced by solvent effects is the indirect formation of the formaldehyde complex **5a** by CH_2O dissociation from the formyl complex **4a** and subsequent recoordination of the formaldehyde molecule. In solution this step is probably facilitated, because the dissociating CH_2O molecule does not leave the solvent cage around the rhodium complex. In this way, the unstable intermediate [HRh(CO)$_3$] (**9a**) does not have to be formed, but a reaction path between direct and indirect formation of **5a** can be followed.

The very high barriers for the formation of the coordinatively unsaturated complexes **7a** and **8a** should also be lowered by solvent effects. The effect is probably somewhat larger for **7a**, because it has a preformed empty coordination site in the trigonal bipyramidal structure, while **8a** has to give up its planar geometry when a solvent molecule is added. Overall, the calculated reaction profile should thus become even smoother under the influence of solvents, because the energy required for the formation of coordinatively unsaturated species can be reduced.

Summary and Conclusions

In the present work the mechanism of the [HRh(CO)$_4$]-catalyzed hydrogenation of carbon monoxide has been studied with the help of systematic ab initio quantum-chemical calculations at the MP2 level of theory. From the available experimental data a proposal for the catalytic mechanism was derived that takes into account the most important intermediates and reaction steps discussed in the literature. Even though the catalytic cycle is not closed yet in the proposed mechanism, the discussion of two reaction channels leading to higher alcohols and methoxy products, respectively, allows a theoretical assessment of the product spectrum of the reaction.

In the first part of the investigation, for each postulated intermediate all the stable conformations were determined and characterized as minima on the potential energy surface by calculation of the energy Hessian. In the geometry optimizations all theoretically reasonable structures were taken into account, and not just those which fit well into the proposed mechanism. Thus, up to 32 starting structures per intermediate had to be considered. Nevertheless, the number of energy minima found was not too large, and in most cases one isomer is clearly the most stable. For the starting catalyst [HRh(CO)$_4$] (**1**) a C_{3v}-symmetrical minimum geometry was calculated, in agreement with the results of IR-spectroscopic studies. For the remaining complexes no experimental data are available, but the calculated structures are chemically very plausible and agree well with the geometries of related complexes.

In the second part of the work, the calculated energy-minimum structures were integrated into the catalytic mechanism. It was found that the most stable isomers of each intermediate are well-matched structurally and that a rather simple and smooth reaction profile results. The calculation of the transition states for the individual reaction steps also yielded only moderate activation barriers. Overall, the calculations thus present a very strong confirmation for the initially proposed mechanism of the catalysis. To our knowledge, this is the first example of such a systematic and unbiased treatment of an organometallic reaction mechanism of this size. However, the presented results confirm the value and even the necessity of this approach.

The calculated reaction mechanism is summarized in Figure 3. The most favourable reaction pathway (Figure 5) starts with the C_{3v}-symmetrical active catalyst [HRh(CO)$_4$] (**1**) that can transform to the formyl complex **2a** by hydride migration to one of the equatorial carbonyl groups. The reaction is strongly endothermic (+28.2 kcal mol^{-1}), but only a small additional barrier of 0.2 kcal mol^{-1} has to be surmounted. Structure **2a** can isomerize to the μ^2-formyl complex **2b**, which can also be formed directly from the starting catalyst **1** with similar energy demand. The subsequent H_2 addition to the equatorial empty coordination site of **2b** takes place without activation energy, but it is only slightly exothermic (−3.3 kcal mol^{-1}). Initially the nonclassical dihydrogen complex **3c** is formed. In the next two slightly exothermic steps, the H_2 ligand is first further attracted to the rhodium centre by rotation of the formyl group (**3b**), and eventually it is oxidatively added yielding the classical dihydrido complex **4a**.

A hydroxycarbene intermediate, frequently discussed in the literature, can be excluded according to our calculations for thermodynamic and kinetic reasons. The competing formation of the side-on formaldehyde complex **5a** is clearly favoured. However, **5a** cannot be directly obtained from the formyl complex **4a**, but only by endothermic dissociation of the CH_2O ligand (+4.9 kcal mol^{-1}) and subsequent barrier-free, strongly exothermic recoordination of the formaldehyde molecule to the planar [HRh(CO)$_3$] complex **9a**. In **5a** the

0947-6539/98/0403-0538 $ 17.50+.50/0 *Chem. Eur. J.* **1998**, *4*, No. 3

hydrogen atom can migrate to the formaldehyde oxygen atom, leading to the hydroxymethyl complex **7a**, which can now react to higher alcohols and their derivatives by further addition of H_2 or CO. The H migration is slightly exothermic (-3.4 kcal mol^{-1}), but has a rather large activation barrier of 17.6 kcal mol^{-1}. The alternative formation of the planar methoxy complex **8a** from the formaldehyde intermediate **5a** is thermodynamically and kinetically only slightly less favourable, so that the observation of methoxy compounds in the product spectrum of the reaction can also be understood.

Overall, a surprisingly simple and rather smooth reaction profile is obtained. The first step of the catalysis, the formation of the formyl complex $[(HCO)Rh(CO)_3]$ from the active catalyst $[HRh(CO)_4]$, is also the rate-determining step of the reaction. It should thus be the reason for the high temperatures and pressures that are necessary in the technical applications. The next question to answer is how this first step might be facilitated, for example by a variation of the ligands. This problem can also be tackled by theoretical methods that investigate the influence of various ligands on the reaction energy and activation barrier of the hydride migration. Work on this as well as on the problem of solvent effects is under way in our group. In the foreseeable future, the rapid progress in method development and computer technology should also permit a further investigation of the next steps of the catalytic mechanism, so that the competing reactions for the building of C_2 products can be compared and eventually the catalytic cycle can be closed.

Supporting information for this paper is available on the WWW under www/wiley-vch.de/home/chemistry, or directly from the author.

Acknowledgements: This work was supported by the Deutsche Forschungsgemeinschaft (SFB 260 and Graduiertenkolleg Metallorganische Chemie) and the Fonds der Chemischen Industrie. We acknowledge the generous support and excellent service provided by the computer centres HRZ Marburg, HHLRZ Darmstadt and HLRZ Jülich. We thank Nikolaus Fröhlich for valuable discussions and assistance in the preparation of the manuscript. U.P. thanks the Fonds der Chemischen Industrie for a doctoral stipend.

Received: August 18, 1997 [F796]

[1] *Applied Homogeneous Catalysis with Organometallic Compounds* (Eds.: B. Cornils, W. A. Herrmann), VCH, Weinheim, **1996**.
[2] L. Markó, *Transition Met. Chem.* **1992**, *17*, 474.
[3] L. Markó, *Transition Met. Chem.* **1992**, *17*, 587.
[4] R. P. A. Sneeden in *Comprehensive Organometallic Chemistry, Vol. 8* (Eds.: E. W. Abel, F. G. A. Stone, G. Wilkinson), Pergamon, Oxford, **1995**.
[5] F. E. Paulik, J. F. Roth, *J. Chem. Soc. Chem. Commun.* **1968**, 1578.
[6] J. R. Blackborow, R. J. Daroda, G. Wilkinson, *Coord. Chem. Rev.* **1982**, *43*, 17.
[7] D. Forster, *Adv. Organomet. Chem.* **1979**, *17*, 255.
[8] A. Spencer, *J. Organomet. Chem.* **1980**, *194*, 113.
[9] H. Dumas, J. Levisalles, H. Rudler, *J. Organomet. Chem.* **1979**, *177*, 239.
[10] R. L. Pruett, *Ann. N.Y. Acad. Sci.* **1977**, *295*, 239.
[11] W. A. Herrmann, *Angew. Chem.* **1982**, *94*, 118; *Angew. Chem. Int. Ed. Engl.* **1982**, *21*, 117.
[12] J. F. Knifton, *J. Am. Chem. Soc.* **1981**, *103*, 3959.
[13] B. D. Dombek, *J. Organomet. Chem.* **1989**, *372*, 151.
[14] a) H. Tanaka, Y. Hara, E. Watanabe, K. Wada, T. Onoda, *J. Organomet. Chem.* **1986**, *312*, C71; b) M. Tamura, M. Ishino, T. Deguchi, S. Nakamura, *J. Organomet. Chem.* **1986**, *312*, C75.
[15] Y. Ohgomori, S. Mori, S. Yoshida, Y. Watanabe, *J. Mol. Catal.* **1987**, *40*, 223.
[16] Y. Kiso, M. Tanaka, T. Hayashi, K. Saeki, *J. Organomet. Chem.* **1987**, *322*, C32.
[17] Y. Hara, E. Watanabe, K. Wada, T. Onoda, *J. Organomet. Chem.* **1989**, *359*, 97.
[18] C. Master, *Adv. Organomet. Chem.* **1979**, *17*, 61.
[19] H. Pichler, H. Schulz, *Chem. Ing. Tech.* **1970**, *42*, 1162.
[20] J. A. Gladysz, *Adv. Organomet. Chem.* **1982**, *20*, 1.
[21] W. Tam, G. Y. Lin, W.-K. Wong, W. A. Kiel, V. K. Wong, J. A. Gladysz, *J. Am. Chem. Soc.* **1982**, *104*, 141.
[22] A. Sisak, E. Sámpár-Szerencsés, V. Galamb, L. Németh, F. Ungváry, G. Pály, *Organometallics* **1989**, *8*, 1096.
[23] a) F. Hutschka, A. Dedieu, W. Leitner, *Angew. Chem.* **1995**, *107*, 1905; *Angew. Chem. Int. Ed. Engl.* **1995**, *34*, 1742; b) F. Hutschka, A. Dedieu, M. Eichenberger, R. Fornika, W. Leitner, *J. Am. Chem. Soc.* **1997**, *119*, 14432.
[24] L. Deng, T. K. Woo, L. Cavallo, P. M. Margl, T. Ziegler, *J. Am. Chem. Soc.* **1997**, *119*, 6177.
[25] a) E. Nakamura, S. Mori, M. Nakamura, K. Morokuma, *J. Am. Chem. Soc.* **1997**, *119*, 4887; b) E. Nakamura, S. Mori, K. Morokuma, *J. Am. Chem. Soc.* **1997**, *119*, 4900.
[26] a) U. Pidun, C. Boehme, G. Frenking, *Angew. Chem.* **1996**, *108*, 3008; *Angew. Chem. Int. Ed. Engl.* **1996**, *35*, 2817; b) M. Stahl, U. Pidun, G. Frenking, *ibid.* **1997**, *109*, 2308 and **1997**, *36*, 2234.
[27] N. Koga, K. Morokuma, *Chem. Rev.* **1991**, *91*, 823.
[28] T. Ziegler, L. Versluis in *Adv. Chem. Ser. 230, Homogeneous Transition Metal Catalyzed Reactions* (Eds.: W. R. Maser, D. W. Slocum), ACS, Washington, **1992**.
[29] P. W. N. M. van Leeuwen, K. Morokuma, J. H. van Lenthe, *Theoretical Aspects of Homogeneous Catalysis*, Kluwer Academic, Dordrecht, **1995**.
[30] D. G. Musaev, K. Morokuma, *Adv. Chem. Phys.* **1996**, *95*, 61.
[31] M. Rosi, A. Sgamellotti, F. Tarantelli, C. Floriani, *J. Chem. Soc. Dalton Trans.* **1988**, 249.
[32] M. R. A. Blomberg, C. A. M. Karlsson, P. E. M. Siegbahn, *J. Phys. Chem.* **1993**, *97*, 9341.
[33] N. Koga, K. Morokuma, *Organometallics* **1991**, *10*, 946.
[34] L. Versluis, T. Ziegler, *J. Am. Chem. Soc.* **1990**, *112*, 6763.
[35] W. Ren-Hu, X. Yin-Sheng, *J. Mol. Catal.* **1989**, *54*, 478.
[36] Z. Xiao-Guang, X. Yin-Sheng, G. Xie-Xian, *J. Mol. Catal.* **1988**, *43*, 381.
[37] H. Zheng Ping, Z. Tian Wei, A. Li Dun, *Chin. Chem. Lett.* **1994**, *5*, 511.
[38] C. Møller, M. S. Plesset, *Phys. Rev.* **1934**, *46*, 618.
[39] K. Fukui, *J. Phys. Chem.* **1970**, *74*, 4161.
[40] K. Fukui, *Acc. Chem. Res.* **1981**, *14*, 363.
[41] C. Gonzalez, H. B. Schlegel, *J. Chem. Phys.* **1989**, *90*, 2154.
[42] C. Gonzalez, H. B. Schlegel, *J. Phys. Chem.* **1990**, *94*, 5523.
[43] C. Gonzalez, H. B. Schlegel, *J. Chem. Phys.* **1991**, *95*, 5853.
[44] a) W. J. Hehre, R. Ditchfield, J. A. Pople, *J. Chem. Phys.* **1972**, *56*, 2257; b) P. C. Hariharan, J. A. Pople, *Theor. Chim. Acta* **1973**, *28*, 213; c) M. S. Gordon, *Chem. Phys. Lett.* **1980**, *76*, 163.
[45] P. J. Hay, W. R. Wadt, *J. Chem. Phys.* **1985**, *82*, 270.
[46] P. J. Hay, W. R. Wadt, *J. Chem. Phys.* **1985**, *82*, 299.
[47] G. Frenking, I. Antes, M. Böhme, S. Dapprich, A. W. Ehlers, V. Jonas, A. Neuhaus, M. Otto, R. Stegmann, A. Veldkamp, S. F. Vyboishchikov in *Reviews in Computational Chemistry, Vol. 8* (Eds.: K. B. Lipkowitz, D. B. Boyd), VCH, New York, **1996**.
[48] a) M. Häser, R. Ahlrichs, *J. Comp. Chem.* **1989**, *80*, 104; b) R. Ahlrichs, M. Bär, M. Häser, H. Horn, M. C. Kölmel, *Chem. Phys. Lett.* **1989**, *162*, 165; c) H. Horn, H. Weiss, M. Häser, M. Ehring, R. Ahlrichs, *J. Comp. Chem.* **1991**, *12*, 1058; d) M. Häser, J. Almlöf, M. W. Feyereisen, *Theor. Chim. Acta* **1991**, *79*, 115; e) A. Schäfer, H. Horn, R. Ahlrichs, *J. Chem. Phys.* **1992**, *97*, 2571; f) M. Häser, R. Ahlrichs, H. P. Baron, P. Weiss, H. Horn, *Theor. Chim. Acta* **1992**, *83*, 455.
[49] M. J. Frisch, G. W. Trucks, M. Head-Gordon, P. M. W. Gill, M. W. Wong, J. B. Foresman, B. G. Johnson, H. B. Schlegel, M. A. Robb, E. S. Replogle, R. Gomperts, J. L. Andres, K. Raghavachari, J. S. Binkley, C. Gonzales, R. L. Martin, D. J. Fox, D. J. Defrees, J. Baker, J. J. P. Stewart, J. A. Pople, *Gaussian 92, Revision C*, Gaussian, Pittsburgh, **1992**.

[50] M. J. Frisch, G. W. Trucks, H. B. Schlegel, P. M. W. Gill, B. G. Johnson, M. A. Robb, J. R. Cheeseman, T. A. Keith, G. A. Petersson, J. A. Montgomery, K. Raghavachari, M. A. Al-Laham, V. G. Zakrzewski, J. V. Ortiz, J. B. Foresman, J. Cioslowski, B. B. Stefanov, A. Nanayakkara, M. Challacombe, C. Y. Peng, P. Y. Ayala, W. Chen, M. W. Wong, J. L. Andres, E. S. Replogle, R. Gomperts, R. L. Martin, D. J. Fox, J. S. Binkley, D. J. Defrees, J. Baker, J. J. P. Stewart, M. Head-Gordon, C. Gonzalez, J. A. Pople, *Gaussian 94, Revision C.2*, Gaussian, Pittsburgh, **1995**.
[51] S. Dapprich, G. Frenking, *J. Phys. Chem.* **1995**, *99*, 9352.
[52] J. L. Vidal, W. E. Walker, *Inorg. Chem.* **1981**, *20*, 249.
[53] V. Jonas, W. Thiel, *J. Chem. Phys.* **1996**, *105*, 3636.
[54] J. S. Dewar, *Bull. Soc. Chim. Fr.* **1951**, *18*, C79.
[55] J. Chatt, L. A. Duncanson, *J. Chem. Soc.* **1953**, 2939.
[56] S. Dapprich, Dissertation, Marburg, **1995**.
[57] G. J. Kubas, R. R. Ryan, B. I. Swanson, P. J. Vergamini, H. J. Wasserman, *J. Am. Chem. Soc.* **1984**, *106*, 451.
[58] J. H. Morris, P. G. Jessop, *Coord. Chem. Rev.* **1992**, *121*, 155.
[59] D. M. Heinekey, W. J. Oldham, Jr., *Chem. Rev.* **1993**, *93*, 913.
[60] U. Pidun, Diplomarbeit, Marburg, **1995**.
[61] U. Pidun, G. Frenking, *Organometallics* **1995**, *14*, 5325.
[62] U. Pidun, G. Frenking, *J. Organomet. Chem.* **1996**, *525*, 269.
[63] G. Frenking, U. Pidun, *J. Chem. Soc. Dalton Trans.* **1997**, 1653.
[64] R. Whyman in ref. [28].
[65] R. Schmid, W. A. Herrmann, G. Frenking, *Organometallics* **1997**, *16*, 701.
[66] G. S. Hammond, *J. Am. Chem. Soc.* **1955**, *77*, 334.
[67] D. Heidrich, W. Kliesch, W. Quapp in *Properties of Chemically Interesting Potential Energy Surfaces*, Springer, Berlin, **1991**.
[68] R. C. Schoehing, J. L. Vidal, R. D. Fiato, *J. Organomet. Chem.* **1981**, *206*, C43.
[69] After finishing this work we carried out additional CCSD(T) calculations of selected MP2-optimized minimum structures and transition states. The essential results of the MP2 calculations remain the same at CCSD(T). The largest differences are found for the initial hydride migration **1** → **2**. The formation of the formyl complex **2b** is less endothermic at CCSD(T) (+21.4 kcal mol^{-1}) than at MP2 (+29.5 kcal mol^{-1}). The energy of the MP2-optimized transition state **TS2** (+20.7 kcal mol^{-1}) is even below the energy of **2b** at the CCSD(T) level. Structure **2b** is predicted to be 5.7 kcal mol^{-1} more stable than **2a** at CCSD(T). This means that the first step of the reaction course (Figures 3 and 5), as calculated at the CCSD(T) level of theory, is the direct formation of **2b**.

  0947-6539/98/0403-0540 $ 17.50+.50/0 *Chem. Eur. J.* **1998**, *4*, No. 3